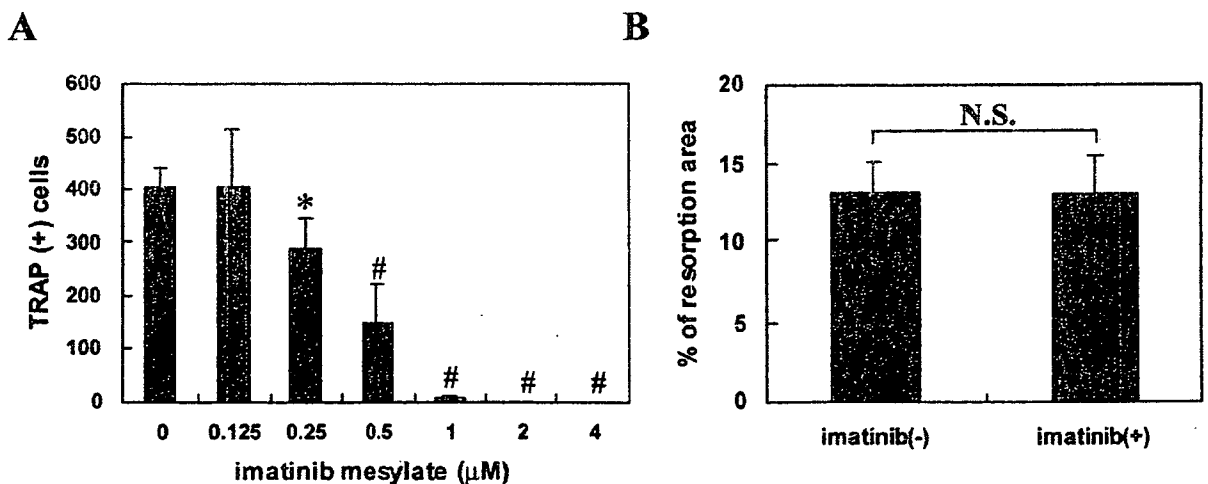


**Fig. 5.** Effect of imatinib mesylate on maintenance of osteoclast precursors. **A** Proliferation assay evaluated by counting the number of rat macrophage colony stimulating factor (M-CSF)-dependent osteoclast precursors (*pre-OC*) or bone marrow cells (*BM cells*) cultured in quadruplicate for 2 days with 0–4 μM imatinib mesylate. Graph shows ratio of cell number relative to controls (0 μM imatinib mesylate). **B** Proliferation evaluated by WST-1 assay of *pre-OC* or *BM cells* cultured in quadruplicate for 2 days with 0–4 μM imatinib mesylate. Graph shows ratio of absorbance relative to controls (0 μM imatinib mesylate). **C** Proliferation evaluated by WST-1 assay of rat osteoclast precursors cultured in quadruplicate for 5 days with 100 ng/ml M-CSF and 0–4 μM imatinib mesylate. Graph shows ratio of absorbance relative to controls (0 μM imatinib mesylate). \**P* < 0.05; \*\**P* < 0.01; #*P* < 0.001 compared with controls (0 μM imatinib mesylate). Bars means ± SD



**Fig. 6.** Effect of imatinib mesylate on osteoclast differentiation and calcified matrix bone resorption by osteoclasts. **A** Numbers of TRAP-positive multinucleate cells (3 or more nuclei, *n* = 4; means ± SD) induced by 100 ng/ml M-CSF and 100 ng/ml soluble receptor activator of NF-κB ligand (sRANKL) together with 0–4 μM imatinib mesylate in quadruplicate. \**P* < 0.05; \*\**P* < 0.01; #*P* < 0.001 compared with 0 μM

imatinib mesylate. **B** Ratio of resorption area to initial surface of hydroxyapatite-coated area at day 10 was not changed compared with that in quadruplicate cultures without imatinib mesylate. Imatinib mesylate (10 μM) was added to medium at day 5 when osteoclasts had differentiated. *N.S.*, not significant. Bars means ± SD

receptor that belongs to the FMS/PDGF receptor family of tyrosine protein kinases. Dewar et al. reported that imatinib mesylate inhibits the development of the monocyte/macrophage lineage from normal human bone marrow progenitors in vitro [30] and subsequently demonstrated that therapeutic concentrations of imatinib mesylate inhibit the phosphorylation of *c-fms* without downregulation of its expression [8]. These data suggest that imatinib mesylate inhibits the maintenance of osteoclast precursors by selectively blocking *c-fms* signaling and subsequently inhibits osteoclastogenesis in pannus as well as bone destruction in CIA rats.

However, this inhibitory effect on osteoclastogenesis and bone destruction was incomplete. Vascular endothelial growth factor (VEGF) as well as M-CSF plays a crucial role in the pathogenesis of inflammatory joint disease, including osteoclastogenesis [31]. Imatinib mesylate does not inhibit ligand-induced phosphorylation of VEGFR1 and VEGFR2 [32]. These findings might explain why osteoclastogenesis was not completely suppressed in vivo in our study. The partial suppression of osteoclastogenesis and the absence of a suppressive effect on the bone resorptive function of differentiated osteoclasts by imatinib mesylate might explain its incomplete suppressive effect on bone destruction.

Imatinib mesylate does not inhibit the tyrosine kinase, src [33,34], which is essential for osteoclast function [35]. Our finding that imatinib mesylate does not influence osteoclastic bone resorption activity is consistent with this fact.

The present study found that the ankle and subtalar joints were more damaged than the MTP joints. This difference might have resulted from the incomplete suppression of joint destruction and a difference in the mechanical stress loaded on these joints. The vertically loaded ankle and subtalar joints might be more susceptible to mechanical destruction than the nonvertically loaded MTP joints.

We found that dexamethasone suppressed synovitis and osteoclastogenesis in CIA rats, although dexamethasone increases osteoclast formation and lacunar resorption in the presence of M-CSF and RANKL in vitro [36]. On the other hand, dexamethasone suppresses the expression of activated NF- $\kappa$ B, which is involved in the inflammation process associated with adjuvant arthritis [37], and proliferating synoviocytes in pannus produce the factors essential for osteoclastogenesis such as M-CSF [20] and RANKL [38]. We therefore considered that the complete inhibition of synovitis with dexamethasone might result in the complete suppression of osteoclastogenesis.

In conclusion, imatinib mesylate prevents joint destruction in CIA rats by reducing osteoclastogenesis at the bone-pannus interface without affecting the inflammatory response. It also inhibited the proliferation of osteoclast precursors that results in a reduction of osteoclastogenesis in vitro. Imatinib mesylate inhibits osteoclastogenesis as well as joint destruction and therefore shows promise as a therapeutic agent against RA.

**Acknowledgment** Work was supported by grants from the Ministry of Health, Labour, and Welfare of Japan.

## References

1. Goldring SR, Gravalles EM (2000) Pathogenesis of bone erosions in rheumatoid arthritis. *Curr Opin Rheumatol* 12:195-199
2. Druker BJ, Tamura S, Buchdunger E, Ohno S, Segal GM, et al. (1996) Effects of a selective inhibitor of the Abl tyrosine kinase on the growth of Bcr-Abl positive cells. *Nat Med* 2:561-566
3. Heinrich MC, Griffith DJ, Druker BJ, Wait CL, Ott KA, et al. (2000) Inhibition of c-kit receptor tyrosine kinase activity by STI 571, a selective tyrosine kinase inhibitor. *Blood* 96:925-932
4. Buchdunger E, Cioffi CL, Law N, Stover D, Ohno-Jones S, et al. (2000) Abl protein-tyrosine kinase inhibitor STI571 inhibits in vitro signal transduction mediated by c-kit and platelet-derived growth factor receptors. *J Pharmacol Exp Ther* 295:139-145
5. Tuveson DA, Willis NA, Jacks T, Griffin JD, Singer S, et al. (2001) STI571 inactivation of the gastrointestinal stromal tumor c-KIT oncoprotein: biological and clinical implications. *Oncogene* 20:5054-5058
6. Miyachi K, Ihara A, Hankins RW, Murai R, Maehiro S, et al. (2003) Efficacy of imatinib mesylate (STI571) treatment for a patient with rheumatoid arthritis developing chronic myelogenous leukemia. *Clin Rheumatol* 22:329-332
7. Eklund KK, Joensuu H (2003) Treatment of rheumatoid arthritis with imatinib mesylate: clinical improvement in three refractory cases. *Ann Med* 35:362-367
8. Dewar AL, Cambareri AC, Zannettino AC, Miller BL, Doherty KV, et al. (2005) Macrophage colony stimulating factor receptor, *c-fms*, is a novel target of imatinib. *Blood* 105:3127-3132
9. van de Wijngaert FP, Tas MC, Burger EH (1989) Conditioned medium of fetal mouse long bone rudiments stimulates the formation of osteoclast precursor-like cells from mouse bone marrow. *Bone (NY)* 10:61-68
10. Felix R, Cecchini MG, Hofstetter W, Elford PR, Stutzer A (1990) Impairment of macrophage colony-stimulating factor production and lack of resident bone marrow macrophages in the osteopetrotic *op/op* mouse. *J Bone Miner Res* 5:781-789
11. Kodama H, Yamasaki A, Nose M, Niida S, Ohgame Y, et al. (1991) Congenital osteoclast deficiency in osteopetrotic (*op/op*) mice is cured by injections of macrophage colony-stimulating factor. *J Exp Med* 173:269-272
12. Tanaka S, Takahashi N, Udagawa N, Tamura T, Akatsu T, et al. (1993) Macrophage colony-stimulating factor is indispensable for both proliferation and differentiation of osteoclast progenitors. *J Clin Invest* 91:257-263
13. Yasuda H, Shima N, Nakagawa N, Yamaguchi K, Kinoshita M, et al. (1998) Osteoclast differentiation factor is a ligand for osteoprotegerin/osteoclastogenesis-inhibitory factor and is identical to TRANCE/RANKL. *Proc Natl Acad Sci U S A* 95:3597-3602
14. Suda T, Takahashi N, Udagawa N, Jimi E, Gillespie MT, et al. (1999) Modulation of osteoclast differentiation and function by the new members of the tumor necrosis factor receptor and ligand families. *Endocr Rev* 20:345-357
15. Udagawa N, Takahashi N, Jimi E, Matsuzaki K, Tsurukai T, et al. (1999) Osteoblasts/stromal cells stimulate osteoclast activation through expression of osteoclast differentiation factor/RANKL but not macrophage colony-stimulating factor: receptor activator of NF- $\kappa$ B ligand. *Bone (NY)* 25:517-523
16. Wood DD, Ihrie EJ, Hamerman D (1985) Release of interleukin-1 from human synovial tissue in vitro. *Arthritis Rheum* 28:853-862
17. Guerne PA, Zuraw BL, Vaughan JH, Carson DA, Lotz M (1989) Synovium as a source of interleukin 6 in vitro. Contribution to local and systemic manifestations of arthritis. *J Clin Invest* 83:585-592
18. Ritchlin C (2000) Fibroblast biology. Effector signals released by the synovial fibroblast in arthritis. *Arthritis Res* 2:356-360
19. Takayanagi H, Iizuka H, Juji T, Nakagawa T, Yamamoto A, et al. (2000) Involvement of receptor activator of nuclear factor  $\kappa$ B ligand/osteoclast differentiation factor in osteoclastogenesis from synoviocytes in rheumatoid arthritis. *Arthritis Rheum* 43:259-269
20. Tsuboi H, Udagawa N, Hashimoto J, Yoshikawa H, Takahashi N, et al. (2005) Nurse-like cells from patients with rheumatoid arthritis support the survival of osteoclast precursors via macrophage-colony stimulating factor production. *Arthritis Rheum* 52:3819-3828

21. Trentham DE, Townes AS, Kang AH (1977) Autoimmunity to type II collagen: an experimental model of arthritis. *J Exp Med* 146:857-868
22. Nishikawa M, Myoui A, Tomita T, Takahi K, Nampei A, et al. (2003) Prevention of the onset and progression of collagen-induced arthritis in rats by the potent p38 mitogen-activated protein kinase inhibitor FR167653. *Arthritis Rheum* 48:2670-2681
23. Cuzzocrea S, Mazzone E, Dugo L, Scerrano I, Britti D, et al. (2001) Absence of endogenous interleukin-10 enhances the evolution of murine type-II collagen-induced arthritis. *Eur Cytokine Netw* 12:568-580
24. Kobayashi K, Takahashi N, Jimi E, Udagawa N, Takami M, et al. (2000) Tumor necrosis factor alpha stimulates osteoclast differentiation by a mechanism independent of the ODF/RANKL-RANK interaction. *J Exp Med* 191:275-286
25. Kirwan JR (1995) The effect of glucocorticoids on joint destruction in rheumatoid arthritis. The Arthritis and Rheumatism Council Low-Dose Glucocorticoid Study Group. *N Engl J Med* 333:142-146
26. Paulus HE, Di Primeo D, Sanda M, Lynch JM, Schwartz BA, et al. (2000) Progression of radiographic joint erosion during low dose corticosteroid treatment of rheumatoid arthritis. *J Rheumatol* 27:1632-1637
27. Perkins SL, Kling SJ (1995) Local concentrations of macrophage colony-stimulating factor mediate osteoclastic differentiation. *Am J Physiol* 269:1024-1030
28. Takeuchi E, Tomita T, Toyosaki-Maeda T, Kaneko M, Takano H, et al. (1999) Establishment and characterization of nurse cell-like stromal cell lines from synovial tissues of patients with rheumatoid arthritis. *Arthritis Rheum* 42:221-228
29. Tomita T, Takeuchi E, Toyosaki-Maeda T, Oku H, Kaneko M, et al. (1999) Establishment of nurse-like stromal cells from bone marrow of patients with rheumatoid arthritis: indication of characteristic bone marrow microenvironment in patients with rheumatoid arthritis. *Rheumatology (Oxf)* 38:854-863
30. Dewar AL, Domasch RM, Doherty KV, Hughes TP, Lyons AB (2003) Imatinib inhibits the in vitro development of the monocyte/macrophage lineage from normal human bone marrow progenitors. *Leukemia* 17:1713-1721
31. Matsumoto Y, Tanaka K, Hirata G, Hanada M, Matsuda S, et al. (2002) Possible involvement of the vascular endothelial growth factor-Flt-1-focal adhesion kinase pathway in chemotaxis and the cell proliferation of osteoclast precursor cells in arthritic joints. *J Immunol* 168:5824-5831
32. Pietras K, Ostman A, Sjoquist M, Buchdunger E, Reed RK, et al. (2001) Inhibition of platelet-derived growth factor receptors reduces interstitial hypertension and increases transcapillary transport in tumors. *Cancer Res* 61:2929-2934
33. Buchdunger E, Cioffi CL, Law N, Stover D, Ohno-John S, et al. (2000) Abl protein-tyrosine kinase inhibitor STI571 inhibits in vitro signal transduction mediated by c-kit and platelet-derived growth factor receptors. *J Pharmacol Exp Ther* 295:139-145
34. Schindler T, Bornmann W, Pellicena P, Miller WT, Clarkson B, et al. (2000) Structural mechanism for STI-571 inhibition of abelson tyrosine kinase. *Science* 289:1938-1942
35. Miyazaki T, Sanjay A, Neff L, Tanaka S, Horne WC, et al. (2004) Src kinase activity is essential for osteoclast function. *J Biol Chem* 279:17660-17666
36. Hirayama T, Danks L, Sabokbar A, Athanasou NA (2002) Osteoclast formation and activity in the pathogenesis of osteoporosis in rheumatoid arthritis. *Rheumatology* 41:1232-1239
37. Tsoo PW, Suzuki T, Totsuka R, Murata T, Takagi T, et al. (1997) The effect of dexamethasone on the expression of activated NF-kappa B in adjuvant arthritis. *Clin Immunol Immunopathol* 83:173-178
38. Romas E, Bakharevski O, Hards DK, Kartsogiannis V, Quinn JM, et al. (2000) Expression of osteoclast differentiation factor at sites of bone erosion in collagen-induced arthritis. *Arthritis Rheum* 43:821-826

# Oxygen Tension Regulates Chondrocyte Differentiation and Function during Endochondral Ossification\*

Received for publication, March 10, 2006, and in revised form, July 13, 2006. Published, JBC Papers in Press, August 11, 2006. DOI 10.1074/jbc.M602296200

Makoto Hirao<sup>‡</sup>, Noriyuki Tamai<sup>‡</sup>, Noriyuki Tsumaki<sup>‡</sup>, Hideki Yoshikawa<sup>‡</sup>, and Akira Myoui<sup>‡§1</sup>

From the <sup>‡</sup>Department of Orthopaedics, Osaka University Graduate School of Medicine, 2-2 Yamadaoka, Suita, Osaka 565-0871, Japan and <sup>§</sup>Medical Center for Translational Research, Osaka University Hospital, 2-15 Yamadaoka, Suita, Osaka 565-0871, Japan

Cartilage functions at a lower oxygen tension than most other tissues. To determine the role of oxygen tension in chondrocyte differentiation and function, we investigated the influence of oxygen tension in the pluripotent mesenchymal cell line C3H10T1/2 and 14.5E mice embryo forelimb organ culture. 10T1/2 cells and embryo forelimbs were cultured under normoxia (20% O<sub>2</sub>) or hypoxia (5% O<sub>2</sub>) in the presence of recombinant human bone morphogenetic protein 2. To elucidate the mechanism by which oxygen tension influences chondrocyte differentiation, the Smad pathway was examined using Smad6 overexpression adenovirus and Smad6 transgenic mice embryo forelimbs. The p38 MAPK pathway was examined using dominant-negative MKK3 and FR167653, a specific p38 MAPK inhibitor. The transcriptional activities of Sox9 and Runx2 were also investigated. Hypoxia promoted bone morphogenetic protein 2-induced glycosaminoglycan production and suppressed alkaline phosphatase activity and mineralization of C3H10T1/2. Thus, hypoxia promoted chondrocytic commitment rather than osteoblastic differentiation. In the mice embryo forelimb organ culture, hypoxia increased cartilaginous matrix synthesis. These effects were primarily mediated by p38 MAPK activation, independent of Sox9. Hypoxia inhibited *Col10a1* (type X collagen  $\alpha$ 1) expression via down-regulation of Runx2 activity by Smad suppression and histone deacetylase 4 activation. In conclusion, hypoxia promotes chondrocytic differentiation and cartilage matrix synthesis and suppresses terminal chondrocyte differentiation. These hypoxia-induced phenomena may act on chondrocytes to enhance and preserve their phenotype and function during chondrocyte differentiation and endochondral ossification.

A number of pathophysiological findings suggest that a correlation exists between hypoxia and chondrogenesis. For example, articular cartilage is an avascular tissue that functions at an oxygen tension that is lower than that of most other tissues. Articular cartilage derives both its nutrition and oxygen supply by diffusion from the synovial fluid and the subchondral bone. It has been estimated that articular chondrocytes in the deepest

layers may have access to no more than 1–6% O<sub>2</sub> (1–6). Furthermore, although the majority of mammalian cells derive their energy by using oxygen for mitochondrial oxidative phosphorylation (7), few mitochondria are present in articular chondrocytes (8). Carbohydrate breakdown in articular cartilage is dominated by the conversion of glucose to lactate via the Embden-Meyerhof-Parnas pathway (9–11) that consumes no O<sub>2</sub>. Similarly, during the endochondral ossification processes that occur in the growth plate, chondromodulin-1, an endogenous inhibitor of neovascularization, is highly expressed by chondrocytes. Of note, most of the growth plate is avascular (12). Recently, in an *in vivo* experiment, it was found that hypoxia-inducible factor 1, which appears to be one of the major regulators of the hypoxic response, is essential for chondrocyte growth arrest and survival (13). Therefore, hypoxia is considered to be a key factor for the growth and survival of chondrocytes. Chondrocytes are derived from undifferentiated mesenchymal cells that have the potential for multidirectional differentiation (14–16). Bone morphogenetic protein (BMP)<sup>2</sup>-2 promotes the chondrocytic differentiation of undifferentiated mesenchymal cells (17–21). BMP-2 activates Smad1-Smad5-Smad8, which subsequently associates with Smad4, relocates to the nucleus, and regulates the expression of target genes (22, 23). However, the influence of oxygen tension on BMP-Smad signaling remains to be elucidated. In addition to the Smad signaling pathway, p38 mitogen-activated protein kinase (p38 MAPK) is also activated by BMP-2 (24, 25). Several other cytokines (26, 27) or stress signals (28–30) can also activate the p38 MAPK pathway. Of particular interest, hypoxia has been found to be one of the stresses that can phosphorylate and activate p38 MAPK (31). Although p38 MAPK has been shown to be implicated in the regulation of chondrogenesis (32–34), the precise role of p38 MAPK in chondrogenesis remains elusive.

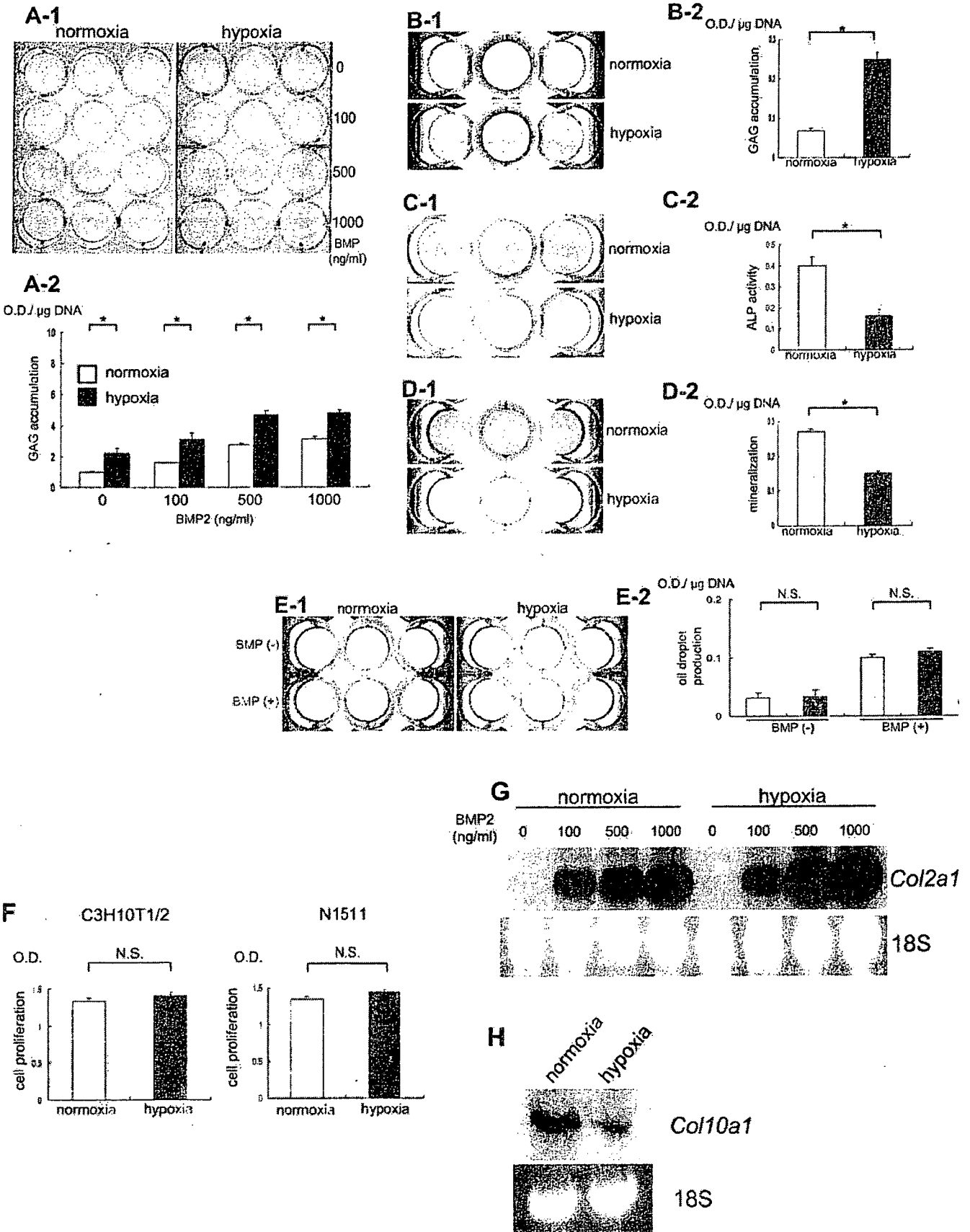
During endochondral ossification, chondrocytes undergo hypertrophy and secrete an extracellular matrix that becomes mineralized and allows vascular invasion and osteoblast differentiation (35, 36). To date, Runx2 and Runx3 (runt-related transcriptional factors 2 and 3) have essential roles in inducing chondrocyte hypertrophy; furthermore, these two interact closely (37–40). In addition, Runx2 is probably a direct tran-

\* This work was supported by Ministry of Education, Culture, Sports, Science, and Technology of Japan Grant 15209050. The costs of publication of this article were defrayed in part by the payment of page charges. This article must therefore be hereby marked "advertisement" in accordance with 18 U.S.C. Section 1734 solely to indicate this fact.

<sup>1</sup> To whom correspondence should be addressed: Medical Center for Translational Research, Osaka University Hospital, 2-15 Yamadaoka, Suita, Osaka 565-0871, Japan. Tel.: 81-6-6879-6551; Fax: 81-6-6879-6549; E-mail: myoi@hp-mctr.med.osaka-u.ac.jp.

<sup>2</sup> The abbreviations used are: BMP, bone morphogenetic protein; MAPK, mitogen-activated protein kinase; HDAC, histone deacetylase; GAG, glycosaminoglycan; WT-Smad6, wild type Smad6; DN-MKK3, dominant negative form of MKK3; ALP, alkaline phosphatase; TK, thymidine kinase; siRNA, small interfering RNA.

Oxygen Tension Regulates Chondrocytes



scriptional activator of chondrocyte maturation. It binds *in vivo* to multiple recognition sites in the *Col10a1* promoter and activates *Col10a1* reporter constructs through these elements *in vitro* (41). Runx2 is also necessary for osteoblast differentiation (42, 43). Runx2 transcriptional activity has been shown to be positively regulated both by the Smad pathway and by the p38 MAPK pathway (44–46). HDAC4, a member of the class II histone deacetylases (HDACs), is expressed in prehypertrophic and hypertrophic chondrocytes and regulates chondrocyte hypertrophy and endochondral bone formation by interacting with Runx2. Recently, HDAC4 has been found to inhibit Runx2 expression by repressing its positive feedback mechanism and inhibiting Runx2 activity (47). Although hypoxia has been shown to down-regulate Runx2 expression in osteoblasts (48), it remains unclear whether Runx2 is involved in the regulation of chondrocyte differentiation and function by oxygen tension.

In the present study, we assessed the influence of oxygen tension on chondrocytic differentiation and cartilage matrix synthesis in the C3H10T1/2 pluripotent mesenchymal cell line and the N1511 murine chondrocyte cell line. We used the mouse embryo organ culture system with wild type mice and Smad6 transgenic mice that we had previously generated. In this paper, we show that hypoxia promotes chondrocytic commitment and cartilage matrix production via the p38 MAPK pathway but that hypoxia inhibits terminal differentiation via the Smad pathway and HDAC4 activation.

## EXPERIMENTAL PROCEDURES

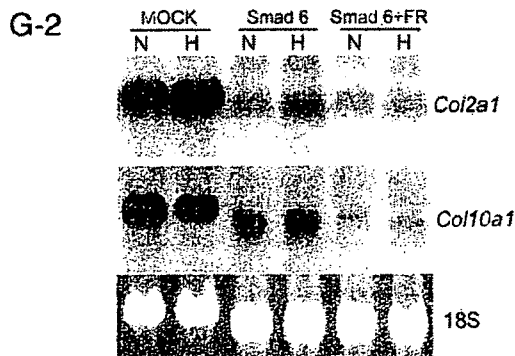
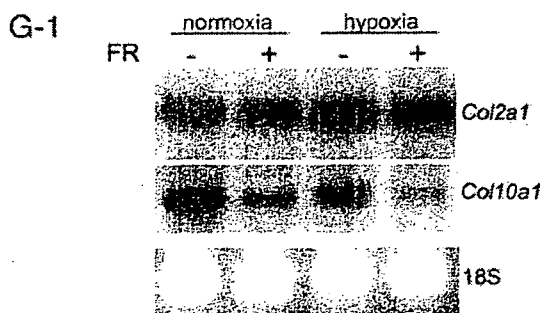
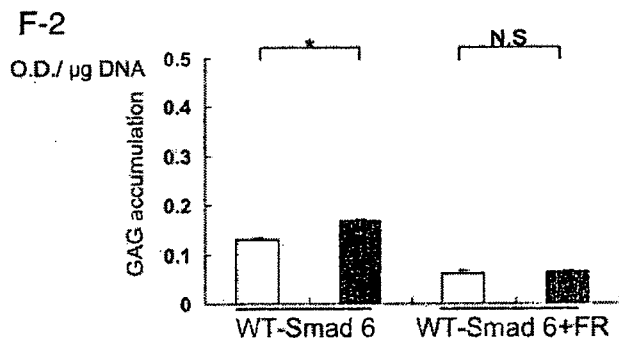
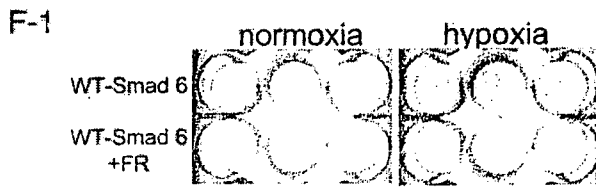
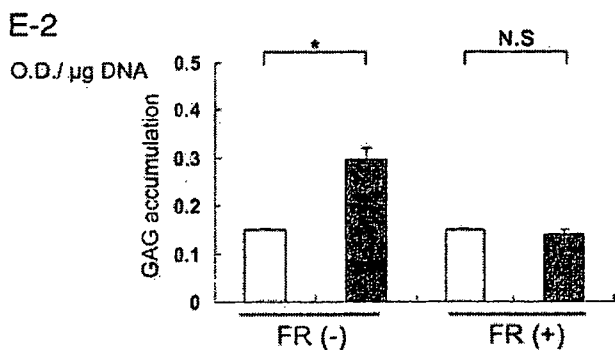
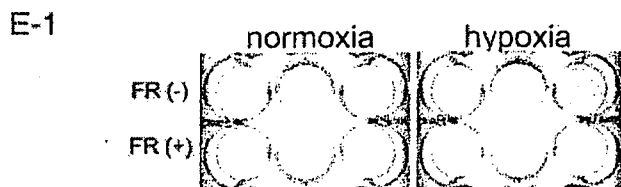
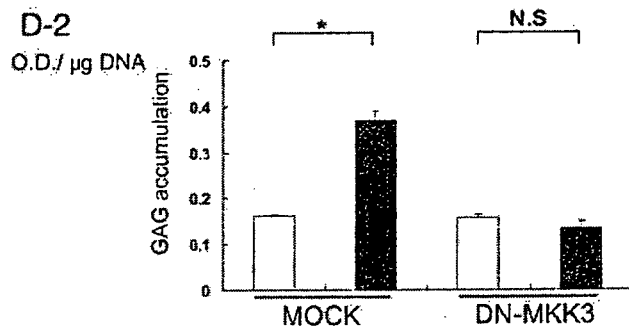
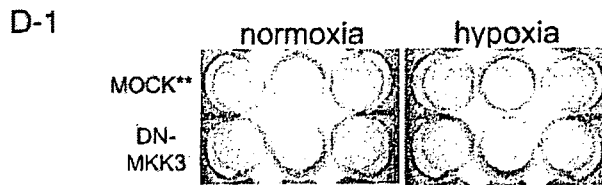
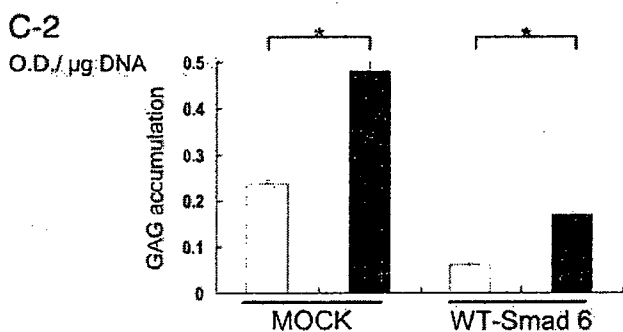
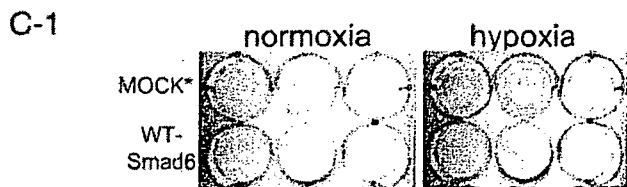
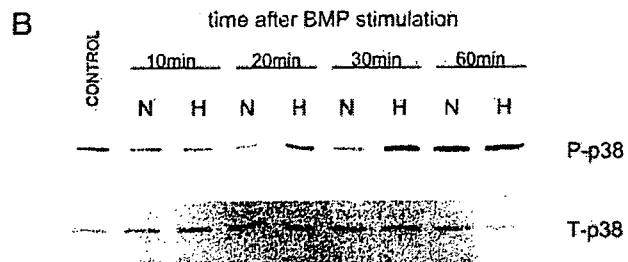
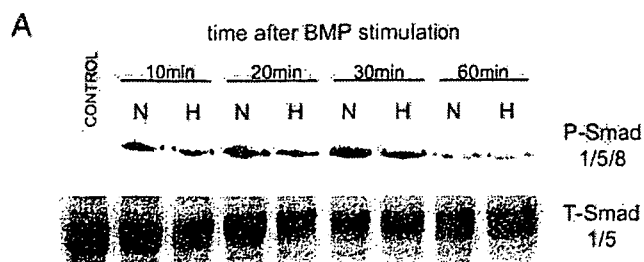
**Cell Culture and Analysis for Chondrocytic, Osteoblastic, and Adipocytic Differentiation**—C3H10T1/2 cells were obtained from RIKEN (Saitama, Japan) and were cultured in Dulbecco's modified Eagle's medium (Invitrogen). Since it has been estimated that articular chondrocytes in the deepest layers may have access to no more than 1–6% O<sub>2</sub>, we selected 5% O<sub>2</sub> as the hypoxic environment for the cells. The cells were incubated at 37 °C under 5% CO<sub>2</sub> and 20% O<sub>2</sub> (normoxia) or 5% CO<sub>2</sub> and 5% O<sub>2</sub> (hypoxia) with or without recombinant human BMP-2. BMP-2 stimulation was added at 90% confluence. To evaluate chondrocytic differentiation, C3H10T1/2 cells were fixed with 10% formalin, washed with distilled water and 0.1 N HCl, and then stained with Alcian blue solution, Alcian blue 8GX (Sigma). We also cultured N1511 murine chondrocytes (49) and stained with Alcian blue. For the quantitative analysis of chondrocytic differentiation, the absorbance of Alcian blue dyes bound to sulfated glycosaminoglycan (GAG) was measured (50). All experiments were performed in triplicate. To

determine osteoblastic differentiation, the C3H10T1/2 cells were fixed with 10% formalin, washed with PBS (pH 7.4) twice, and incubated with alkaline phosphatase (ALP) substrate solution, 0.1 mg/ml naphthol AS-MX (Sigma), and 0.6 mg/ml fast violet B salt (Sigma) in 0.1 M Tris-HCl, pH 8.5. The activity of ALP was also measured using an ALP test kit (Wako, Osaka, Japan) according to the manufacturer's instruction. To evaluate matrix mineralization, the cultures were stained with alizarin red solution (Sigma) (pH 6.0) and incubated in 100 mM cetylpyridinium chloride for 1 h to solubilize and release calcium-bound alizarin red S into solution. The absorbance of the released alizarin red S was measured (51). To determine adipocytic differentiation, the C3H10T1/2 cells were fixed in 10% formalin, washed with diluted water and 60% isopropyl alcohol, and stained with Oil red O (Sigma) solution. Quantitative analysis for oil droplet was performed as described previously (52). To measure the value of absorbance for alcian blue, alizarin red, and oil red O relative to cell density, the absorbance data were normalized by total DNA content. Total DNA content was extracted using a DNeasy tissue kit (Qiagen, Düsseldorf, Germany) and measured. Cell proliferation analysis was also performed. C3H10T1/2 and N1511 cells were cultured in flat bottomed 96-well microplates at a concentration of  $1 \times 10^4$  cells/ml in Dulbecco's modified Eagle's medium containing 10% fetal bovine serum. After 7 days, cell viability was assessed by cell proliferation assay system kit (Takara Bio Inc., Otsu, Japan), using the sulfonated tetrazolium salt 2-(4-iodophenyl)-3-(4-nitrophenyl)-5-(2,4-disulfophenyl)-2H-tetrazolium monosodium (WST-1).

**Organ Culture of Embryonic Limb Explants**—The forelimbs from embryonic day 14.5 embryos of ICR wild type mice (Charles River, Osaka, Japan) and Smad6-overexpressing transgenic mice (53) were stripped of skin and muscles. They were then cultured for 5 days in BGG-B medium (Invitrogen) with 1% penicillin/streptomycin (Invitrogen) and 0.1% fetal bovine serum in organ culture dishes under humidified conditions as previously reported (54–56). Cultures were supplemented with 500 ng/ml BMP-2 under normoxia or hypoxia. After 5 days, limb explants were fixed overnight in 4% paraformaldehyde at 4 °C and embedded in paraffin. Serial 3- $\mu$ m-thick sections from the wild type mice ( $n = 6$ ) and the transgenic mice ( $n = 5$ ) were processed for safranin O staining and *in situ* hybridization. Briefly, sections were stained with hematoxylin (Sigma) and fast green (Merck) to identify cells and with safranin-O (Sigma) to identify GAGs.

**FIGURE 1. Hypoxia promotes chondrocytic differentiation and GAG production, whereas it suppresses osteoblastic differentiation and chondrocyte terminal differentiation in C3H10T1/2 cell culture.** A, C3H10T1/2 cells were cultured with BMP-2 (0, 100, 500, or 1000 ng/ml) under normoxia or hypoxia for 7 days. A-1, the cells were stained with alcian blue. A-2, BMP-2 induced GAG production in a dose-dependent manner. Data are shown as mean  $\pm$  S.E. ( $n = 3$ ) OD/ $\mu$ g of DNA. \*,  $p < 0.01$ . B, N1511 cells were cultured with 100 ng/ml BMP-2 for 8 days. B-1, the cells were stained with alcian blue. B-2, quantification of GAG synthesis by N1511 cells. Data were normalized by total DNA content. Data are shown as mean  $\pm$  S.E. ( $n = 3$ ) OD/ $\mu$ g of DNA. \*,  $p < 0.001$ . C, C3H10T1/2 cells were cultured with 500 ng/ml BMP-2 for 7 days. The cells were then stained for ALP activity (C-1). C-2, quantification of ALP activity. Data are shown as mean  $\pm$  S.E. ( $n = 6$ ) OD/ $\mu$ g of DNA. \*,  $p < 0.01$ . D-1, C3H10T1/2 cells were cultured with 500 ng/ml BMP-2 for 8 days. The cells were then stained with alizarin red solution. D-2, quantification of matrix mineralization. Data were normalized by total DNA content. Data are shown as mean  $\pm$  S.E. ( $n = 3$ ) OD/ $\mu$ g of DNA. \*,  $p < 0.001$ . E-1, C3H10T1/2 cells were cultured with or without BMP-2 (500 ng/ml) for 7 days. The cells were stained with oil red O staining solution. E-2, quantification of oil droplet production. Data were normalized by total DNA content. Data are shown as mean  $\pm$  S.E. ( $n = 3$ ) OD/ $\mu$ g of DNA. N.S., not significant;  $\square$ , normoxia;  $\blacksquare$ , hypoxia. F, cell proliferation analysis was performed 7 days after the culture, as described under "Experimental Procedures." Data are shown as mean  $\pm$  S.E. ( $n = 12$ ). \*,  $p < 0.05$ ; N.S., not significant. G, C3H10T1/2 cells were cultured with BMP-2 for 7 days, total RNA was extracted, and Northern blotting analysis was done for *Col2a1* genes (10  $\mu$ g of total RNA/lane). Expression of 18 S was used to control the amount of RNA. H, C3H10T1/2 cells were cultured with 500 ng/ml BMP-2 for 7 days. Total RNA was extracted and subjected to Northern blotting analysis for the *Col10a1* gene.

# Oxygen Tension Regulates Chondrocytes



Computer-assisted histological analysis for the proportion of the GAG production area per whole radius was performed using a Nikon ECLIPSE E1000 microscope with a Plan Apo objective, combined with a Nikon DXM 1200 Digital Camera (Tokyo, Japan) and WinRoof image processing software (Mitani Corp.) for Windows. Digitized pictures taken for each radius were analyzed to calculate the ratio of the area stained with safranin-O per whole radius. *In situ* hybridization for *Col10a1* was done as described previously (53, 57). The proportional length of the hypertrophic positive signal of *Col10a1* with respect to the whole hypertrophic chondrocyte zone along the midline was calculated. The care and handling of the animals and the procedures used in this study were in accordance with the guidelines of and were approved by the Osaka University Medical School Animal Care and Use Committee.

**Antibodies and Reagents**—Anti-phospho-Smad 1/5/8 monoclonal antibody, anti-phospho-p38 MAPK polyclonal antibody, and anti-p38 MAPK monoclonal antibody were purchased from Cell Signaling Technology (Beverly, MA). Anti-Smad 1/5 polyclonal antibody was purchased from Calbiochem. Anti-Sox9 antibody was purchased from Chemicon (Temecula, CA). Anti-HDAC4, anti- $\beta$ -actin, and antiproliferating cell nuclear antigen polyclonal or monoclonal antibody was purchased from Santa Cruz Biotechnology, Inc. (Santa Cruz, CA). Alexa Fluor<sup>®</sup> 488 goat anti-rabbit IgG (H + L) antibody was purchased from Molecular Probes, Inc. (Eugene, OR). Hoechst 33342 solution was purchased from Dojindo (Kumamoto, Japan). Recombinant human BMP-2 and a potent p38 MAPK inhibitor, FR167653, were provided by Astellas Pharmaceutical Co., Ltd. (Osaka, Japan).

**DNA Constructs**—Wild type Smad6 (WT-Smad6)-expressing adenovirus and the dominant negative form of MKK3 (DN-MKK3) vector were donated by Dr. Riko Nishimura (Department of Biochemistry, Osaka University Graduate School, Faculty of Dentistry). Wild type Runx2-expressing vector was donated by Dr. Toshihisa Komori (Department of Developmental and Reconstructive Medicine, Division of Oral Cytology and Cell Biology, Nagasaki University Graduate School of Biomedical Sciences).

**Reporter Constructs and Luciferase Reporter Assay**—Four tandems of 48-bp chondrocyte-specific enhancer segments of type II collagen  $\alpha 1$  (*Col2a1*) were synthesized as previously reported (58) and inserted into the PGL3 promoter

vector (Promega), 4Col2E-Luc. Six tandems of the Runx2 binding site were also inserted into the PGL3 promoter vector (Promega), 6Runx2E-Luc. Reporter assays were performed by transient transfection of 0.4  $\mu$ g of the PGL3-promoter vector (4Col2E-Luc or 6Runx2E-Luc) and 0.01  $\mu$ g of the TK-*Renilla* luciferase construct (TK *Renilla*) (Promega). Luciferase activity was measured using a Dual Luciferase assay kit (Promega) and luminometer (Berthold Technologies, Bad Wildbad, Germany) and normalized by determining the activity of *Renilla* luciferase. All experiments were performed in triplicate.

**RNA Interference**—RNA interference was done using commercially synthesized siRNA (Qiagen, Düsseldorf, Germany) and used as described in the protocols provided by the manufacturer. Cells were treated with siRNA to a final concentration of 10  $\mu$ M. The siRNA duplex sequence targeting the HDAC4 protein was aagucagcagcgaagautt (sense strands), as previously described (59). Control siRNA consisted of siRNA targeted against luciferase (Dharmacon, Lafayette, CO).

**Phosphorylation of Sox9**—Serine/threonine phosphorylation of Sox9 was analyzed by affinity chromatography using a phosphoprotein purification kit (Qiagen). Cells were lysed using the lysis buffer provided in the kit. The extracted protein was applied to a phosphorylation purification column, and phosphorylated protein was eluted. Unphosphorylated protein was obtained from the flow-through fraction. These samples were blotted with anti-Sox9 antibody.

**Western Blot Analysis**—Western blot analyses were performed using whole cell lysates. To detect HDAC4 protein, nuclear extracts were obtained as previously reported (60). The MC3T3-E1 cell (mouse osteoblastic cell) was used as a control. The blots were first incubated with appropriate antibodies and then with horseradish peroxidase-coupled anti-mouse or rabbit IgG antibodies (Amersham Biosciences). For the blots, 20  $\mu$ g of each sample was applied.

**Northern Blot Analysis**—Total RNA was isolated from C3H10T1/2 cells using the RNeasy kit (Qiagen). The blots were hybridized with probes for *Col2a1*, *Col10a1*, *Sox9*, and *Runx2* mRNA. <sup>32</sup>P-Radiolabeled DNA probes were synthesized using cDNA obtained from reverse transcriptase-PCR amplification. The following primers were used: *Col2a1* (forward primer, 5'-CCTGTCTGCTTCTTGTA AAC-3'; reverse primer, 5'-AAAAAATACAGAGGTGTTTGACACAGA-3'), *Col10a1* (forward primer, 5'-AATCTCATAAATGGGATGGG-3';

**FIGURE 2. Hypoxia-induced GAG production and *Col2a1* gene expression are mediated by the p38 MAPK pathway rather than the Smad pathway.** A and B, C3H10T1/2 cells were cultured with or without BMP-2 (500 ng/ml) under normoxia or hypoxia for 10, 20, 30, and 60 min and lysed. The cell lysates were determined by Western blotting with anti-phospho-Smad1-Smad5-Smad8 (P-Smad 1/5/8) or anti-Smad1-Smad5 (T-Smad 1/5) antibodies (A) and with anti-phospho p38 MAPK (P-p38) or anti-p38 MAPK (T-p38) antibodies (B). N, normoxia; H, hypoxia. C–F, regulatory mechanisms of GAG production by hypoxia. □, normoxia; ■, hypoxia. C, 12 h after infection with WT-Smad6 adenovirus (WT-Smad6), C3H10T1/2 cells were stimulated with BMP-2 (500 ng/ml) and incubated under normoxia or hypoxia. LacZ expression adenovirus (MOCK\*) was used as a control. C-1, after 7 days, the cells were stained with alcian blue. D, 24 h after transfection with DN-MKK3, C3H10T1/2 cells were stimulated with BMP-2 (500 ng/ml). pGL3 promoter vector (MOCK\*\*) was used as a control. D-1, after 5 days, the cells were stained with alcian blue. E, C3H10T1/2 cells were stimulated with BMP-2 (500 ng/ml) in the presence or absence of the p38 MAPK inhibitor, FR167653 (1  $\mu$ M). The media were changed every 3 days for completely fresh media containing BMP-2 in the presence or absence of FR167653. FR, FR167653. E-1, after 7 days, the cells were stained with alcian blue. F, 12 h after infection with WT-Smad6 adenovirus, C3H10T1/2 cells were stimulated with BMP-2 (500 ng/ml) in the presence or absence of the p38 MAPK inhibitor, FR167653 (1  $\mu$ M). F-1, after 7 days, the cells were stained with alcian blue. C-2, D-2, E-2, and F-2, the absorbance of alcian blue dye bound to GAG in each well was quantified (OD/ $\mu$ g of DNA). Data are shown as mean  $\pm$  S.E. (n = 3) (OD/ $\mu$ g of DNA). \*, p < 0.01; N.S., not significant. G, regulatory mechanisms of *Col2a1* and *Col10a1* gene expression by hypoxia. G-1, C3H10T1/2 cells were cultured for 5 days with 500 ng/ml BMP-2 in the absence or presence of 1  $\mu$ M FR167653. Northern blotting analysis for *Col2a1* and *Col10a1* genes was performed (10  $\mu$ g of total RNA/lane). G-2, 12 h after infection with WT-Smad6 adenovirus, the cells were incubated with BMP-2 (500 ng/ml) in the absence or presence of 1  $\mu$ M FR167653. LacZ expression adenovirus (MOCK) was used as a control. Northern blotting analysis for *Col2a1* and *Col10a1* was performed. N, normoxia; H, hypoxia.



# Oxygen Tension Regulates Chondrocytes

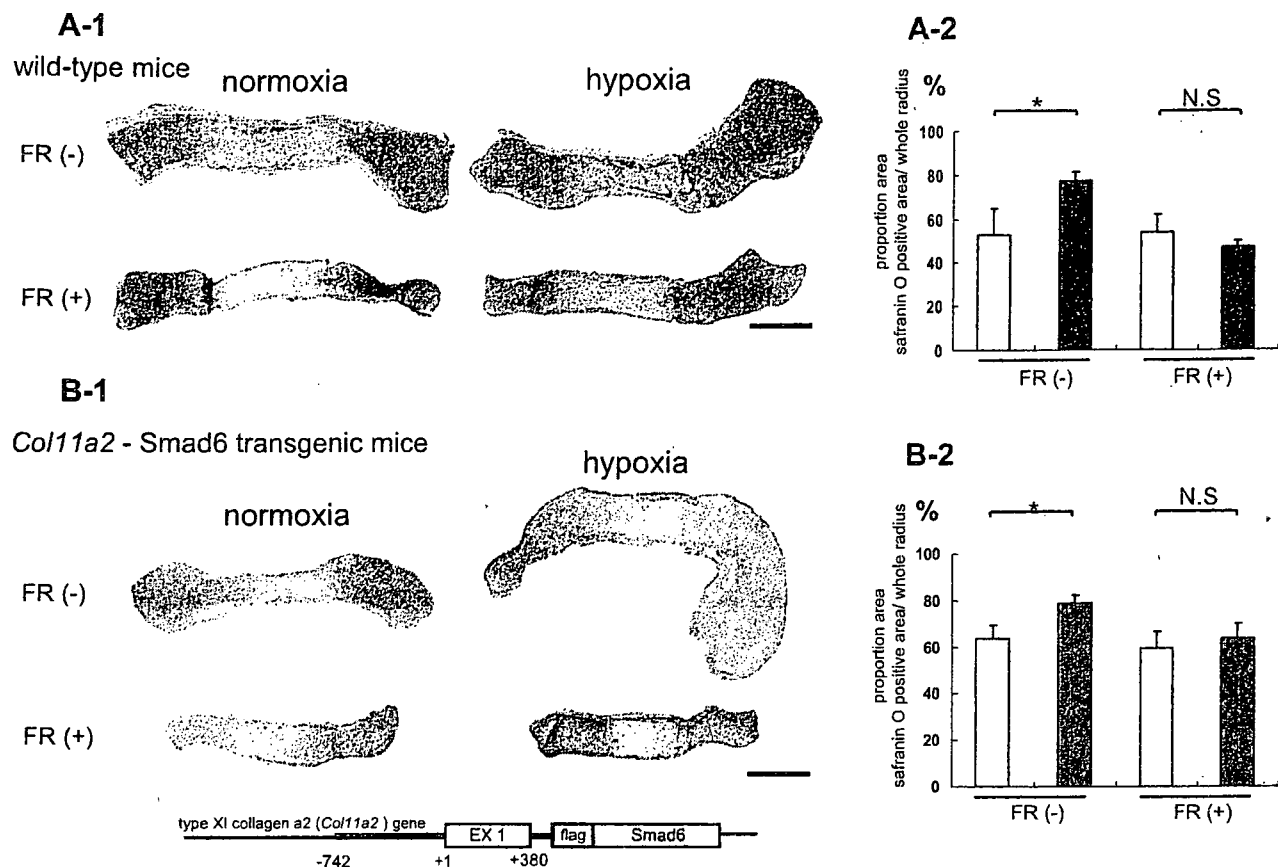


**FIGURE 3. Hypoxia enlarges the cartilaginous matrix area via the p38 MAPK pathway in organ culture system.** A, normal mouse embryo forelimb organ culture with BMP-2 (500 ng/ml). A-1, histology of the radius of a normal mouse embryo (embryonic day 14.5) visualized with safranin O/fast green/iron hematoxylin staining. FR(+), 1  $\mu$ M FR167653. A-2, morphometric analysis of the forelimb explants. The proportion of the area stained with safranin O per whole radius was measured for each section as described under "Experimental Procedures." Data are shown as mean  $\pm$  S.E. (n = 6). \*, p < 0.05; N.S., not significant.  $\square$ , normoxia;  $\blacksquare$ , hypoxia. B, Smad6 transgenic mouse embryo forelimb organ culture. B-1, histology of the radius of a Smad6 transgenic mouse embryo (embryonic day 14.5). B-2, morphometric analysis of forelimb explants. Data are shown as mean  $\pm$  S.E. (n = 5). \*, p < 0.05; N.S., not significant.  $\square$ , normoxia;  $\blacksquare$ , hypoxia. Bars, 240  $\mu$ m.

reverse primer, 5'-CCTGGGTTAGATGGAAAA-3'), Sox9 (forward primer, 5'-ATGAATCTCCTGGACCCCTT-3'; reverse primer, 5'-AACTTGGCCAGCTTGCACGT-3'), Runx2 (forward primer, 5'-GCTTGATGACTCTAAACCTA-3'; reverse primer, 5'-AAAAAGGGCCCAGTTCTGAA-3'). PCR products were purified using the PCR purification kit (Qiagen).

**Reverse Transcription PCR Analysis**—First-strand cDNA was synthesized using SuperScript II RNase H<sup>-</sup> reverse transcriptase (Invitrogen). The PCR was performed using Ex Taq (Takara Bio Inc., Otsu, Japan). The primers for the Runx2 gene were the same as those used for Northern blotting. The GAPDH primers included the forward primer (5'-TGAACGGGAAGCTCACTGG-3') and the reverse primer (5'-TCCACCACCCTGTTGCTGTA-3').

**Quantitative Real Time PCR Analysis**—We obtained cDNA by reverse transcription as mentioned above and proceeded with real time PCR using the Roche Applied Science Light Cycler<sup>®</sup> system. The SYBR<sup>®</sup> Green assay, in which each cDNA sample was evaluated in triplicate 20- $\mu$ l reactions, was used for all target transcripts. Expression values were normalized to GAPDH. The primers for the Runx2 and GAPDH genes were the same as above. The Sox9 primers

were as follows: forward, 5'-ATGAATCTCCTGGACCCCTT-3'; reverse, 5'-TTGGGGAAGGTGTTCTCCT-3'.

**Statistical Analysis**—All data are expressed as mean  $\pm$  S.E. Differences between groups were assessed using Student's t test, and differences among three or more groups were assessed by *post hoc* testing. A p value of <0.05 was considered statistically significant.

## RESULTS

**Hypoxia Promotes Chondrocytic Differentiation and GAG Production, whereas It Suppresses Osteoblastic Differentiation and Chondrocyte Terminal Differentiation in C3H10T1/2 Cell Culture**—In C3H10T1/2 cell culture, BMP-2 induced GAG production in a dose-dependent manner (Fig. 1A). At every BMP-2 concentration tested, hypoxia clearly increased GAG content additively with BMP-2. Hypoxia-induced GAG synthesis was also found in the N1511 murine chondrocyte culture (Fig. 1B). On the other hand, low oxygen tension clearly suppressed ALP activity and alizarin red staining of C3H10T1/2 cells (Fig. 1, C and D), suggesting that hypoxia suppressed BMP-2-induced osteoblastic differentiation. Adipocytic differentiation, as identified by oil red O staining, was not affected by

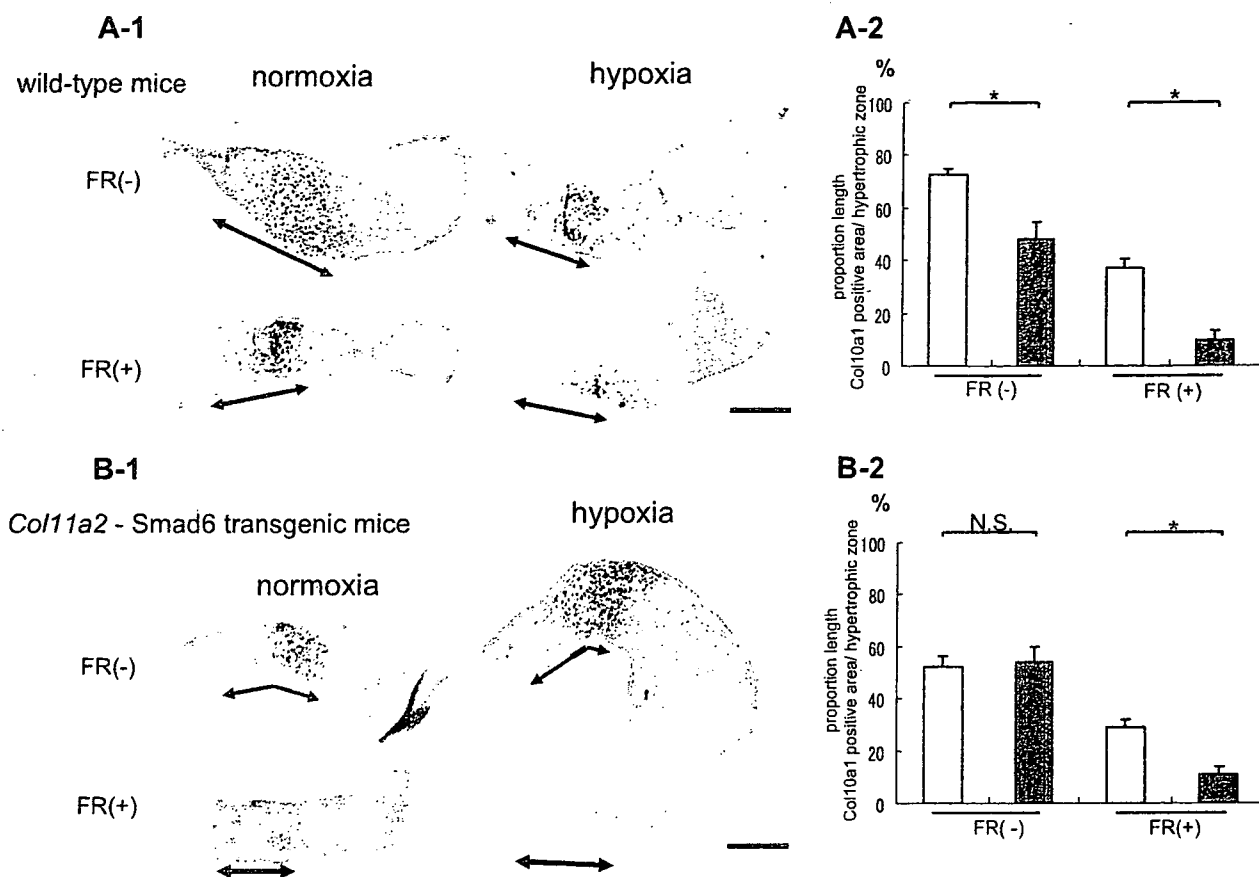


**FIGURE 4. Terminal differentiation of chondrocytes is suppressed by hypoxia in mouse embryo organ cultures.** *A*, normal mouse embryo forelimb organ culture. *A-1*, sections of normal mice forelimbs were hybridized with cRNA probes for *Col10a1*. FR(+), 1  $\mu$ M FR167653. *A-2*, the proportion of the length of *Col10a1* mRNA expression site per hypertrophic chondrocyte zone (bidirectional arrow) along the midline was measured for each section. Data are shown as mean  $\pm$  S.E. ( $n = 6$ ). \*,  $p < 0.05$ ; \*\*,  $p < 0.01$ ;  $\square$ , normoxia;  $\blacksquare$ , hypoxia. *B*, Smad6 transgenic mouse embryo forelimb organ culture. *B-1*, sections of Smad6 transgenic mouse forearms were hybridized with cRNA probes for *Col10a1*. *B-2*, morphometric analysis of the forelimb explants. Data are shown as mean  $\pm$  S.E. ( $n = 5$ ). \*,  $p < 0.05$ ; N.S., not significant;  $\square$ , normoxia;  $\blacksquare$ , hypoxia. Bars, 120  $\mu$ m.

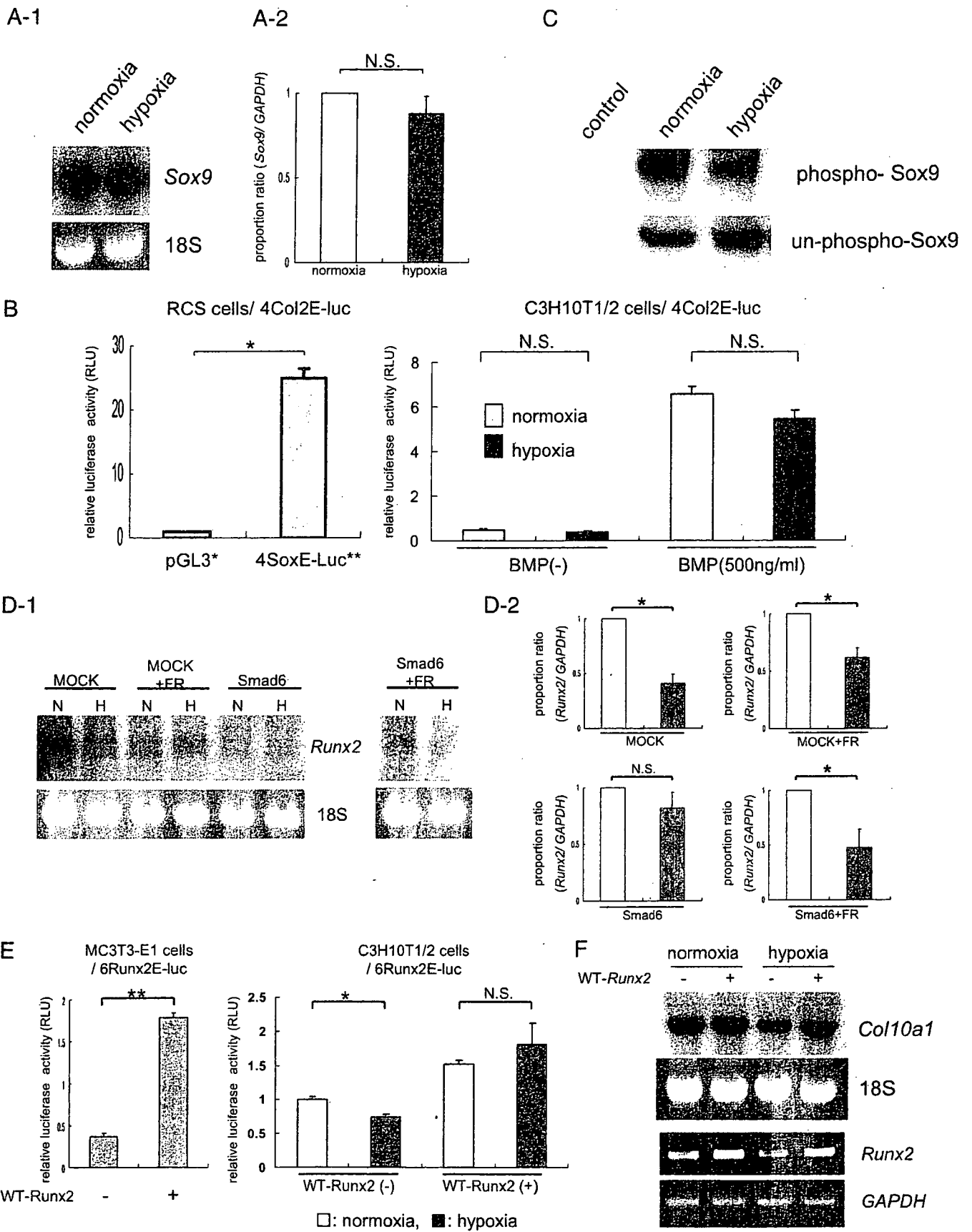
oxygen tension (Fig. 1E). After cell proliferation became confluent, there was no difference of the cell proliferation between normoxia and hypoxia at 7 days in C3H10T1/2 cells and N1511 cells (Fig. 1F). The type II collagen  $\alpha 1$  (*Col2a1*) gene, a well characterized, specific marker of commitment to the chondrogenic lineage, was up-regulated by BMP-2 in a dose-dependent manner (Fig. 1G) as well as by hypoxia at each BMP-2 concentration tested. The mRNA expression of the type X collagen  $\alpha 1$  (*Col10a1*) gene, a well characterized, specific marker for chondrocyte terminal differentiation (61, 62), was suppressed by hypoxia (Fig. 1H), in contrast to *Col2a1* mRNA expression.

**Hypoxia-induced GAG Production Is Mediated by the p38 MAPK Pathway rather than the Smad Pathway**—To investigate the intracellular signal transduction mechanisms responsible for hypoxia-induced chondrocyte differentiation, we first examined the activities of the Smad and the p38 MAPK pathways. As shown in Fig. 2, *A* and *B*, phosphorylation of p38 MAPK is up-regulated by hypoxia, whereas phosphorylation of Smad is down-regulated. When Smad signaling was inhibited by the overexpression of WT-Smad6, which inhibits phosphorylation of the Smad1-Smad5-Smad8 complex, BMP-2-induced GAG production was markedly reduced under both oxygen levels. However, hypoxia was still able to promote GAG

production despite Smad inhibition (Fig. 2C). In contrast, hypoxia-induced GAG production was abolished by the overexpression of DN-MKK3 that specifically inhibits p38 MAPK phosphorylation (Fig. 2D) and also by FR167653, a specific p38 MAPK inhibitor (Fig. 2E). When both the Smad and the p38 MAPK pathways were blocked by Smad6 overexpression and FR167653, hypoxia did not influence the GAG production level (Fig. 2F).

**Regulatory Mechanisms of *Col2a1* and *Col10a1* Gene Expression by Oxygen Tension**—Next, we assessed the role of the p38 MAPK and Smad pathways in the regulation of *Col2a1* and *Col10a1* gene expression. In the presence of FR167653, hypoxia-induced *Col2a1* expression was suppressed (Fig. 2, G-1). However, when WT-Smad6 was overexpressed, although *Col2a1* gene expression was suppressed under both oxygen conditions, hypoxia strongly induced the *Col2a1* gene. When both Smad and p38 MAPK signaling was blocked by WT-Smad6 and FR167653, *Col2a1* gene induction caused by hypoxia was again strongly attenuated (Fig. 2, G-2). Our findings suggest that hypoxic regulation of *Col2a1* gene expression is mediated by the p38 MAPK pathway rather than the Smad pathway, which is very similar to the mechanism of hypoxic regulation involved in GAG production. On the other hand,

Oxygen Tension Regulates Chondrocytes



*Col10a1* gene expression was reduced by hypoxia as shown in Fig. 1G, and it seemed to be regulated in a complicated manner that is different from *Col2a1* gene expression. The blockade of the p38 MAPK pathway did not alter the hypoxia-related reduction of *Col10a1* gene expression, but the blockade of the Smad pathway abolished it. However, when both pathways were blocked, hypoxia reduced *Col10a1* gene expression (Fig. 2G).

**Hypoxia Enlarges the Cartilaginous Matrix Area Associated with Endochondral Ossification via the p38 MAPK Pathway in Organ Culture**—Our data show that hypoxia promoted the commitment of C3H10T1/2 cells to a chondrocytic lineage and enhanced cartilage matrix production via the p38 MAPK pathway. To further confirm the influence of oxygen tension on cartilage biology in a setting similar to that found *in vivo*, we cultured embryonic day 14.5 embryo forelimbs obtained from wild type and Smad6 transgenic mice. In *ex vivo* embryo limb cultures in the presence of BMP-2, explants grew quickly both in length and in width and wound greatly as they grow. Therefore, to evaluate cartilaginous matrix production, we calculated the proportion of the area of each radius that was stained with safranin-O compared with the whole radius area. The embryo forelimbs that were cultured under hypoxic conditions showed a significantly greater enlargement in the matrix area, and hypoxia-induced cartilage enlargement was abolished by FR167653 (Fig. 3, A-1). In explants from Smad6 transgenic mice, hypoxia enlarged the cartilage matrix area, and FR167653 abolished hypoxia-induced matrix enlargement (Fig. 3, B-1). These findings are consistent with our *in vitro* observation that hypoxia promotes cartilaginous matrix synthesis not via the Smad pathway but via p38 MAPK signaling (Fig. 2G).

**Terminal Differentiation of Chondrocyte Is Suppressed by Hypoxia in Mouse Embryo Organ Cultures**—In C3H10T1/2 cell cultures, *Col10a1* gene expression was repressed by hypoxia. In accordance with this, when using *in situ* hybridization, we found that, in wild type embryo forelimb cultures, hypoxia reduced the *Col10a1* gene expression level estimated by the proportional length of the *Col10a1*-positive site per whole hypertrophic chondrocyte zone (Fig. 4, bidirectional arrows) along the midline. When p38 MAPK signaling was suppressed using FR167653, the *Col10a1*-positive area was markedly reduced with both oxygen levels. In addition, hypoxia apparently reduced the *Col10a1*-positive area regardless of the use of p38 MAPK inhibitor (Fig. 4A). On the other hand, hypoxia alone did not repress *Col10a1* gene expression in Smad6 trans-

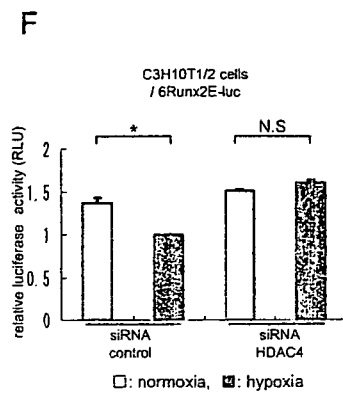
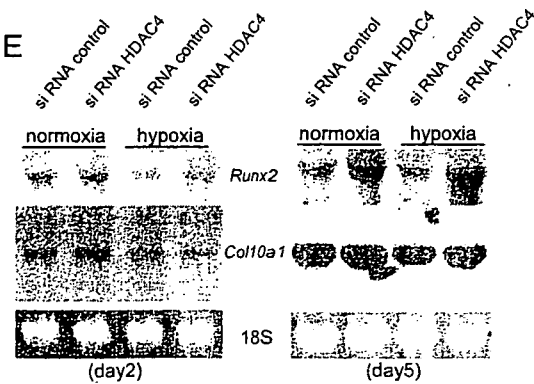
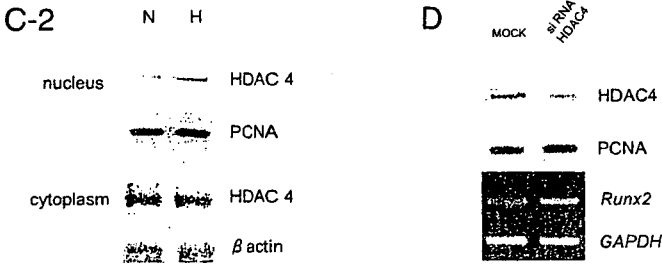
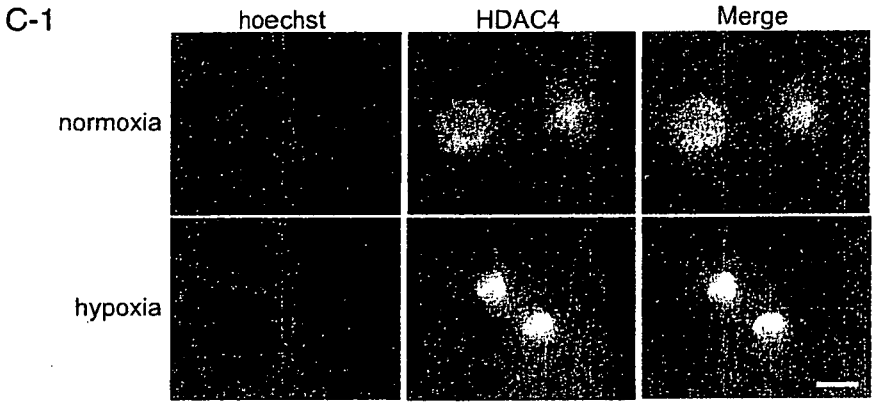
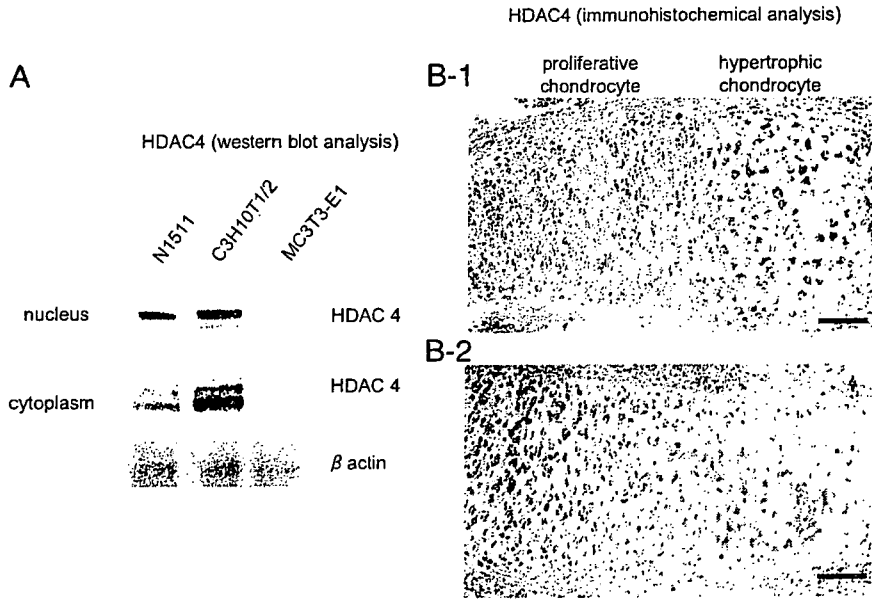
genic mice embryo forelimb organ culture, although hypoxia did suppress *Col10a1* gene expression when the p38 MAPK pathway was inhibited by FR167653 (Fig. 4B). These findings were in agreement with the *in vitro* results and suggest that the Smad pathway mediates *Col10a1* gene down-regulation and that the p38 MAPK pathway mediates its up-regulation. In addition, hypoxia reduced *Col10a1* expression even when both Smad and p38 MAPK signaling were blocked, which would suggest that unknown factors that down-regulate *Col10a1* gene expression are involved.

**Sox9 Gene Expression and Its Transcriptional Activity Are Not Up-regulated by Hypoxia**—Sox9 is a key transcriptional factor for chondrocytic differentiation and regulates transcription of the *Col2a1* gene. Thus, we evaluated the influence of oxygen tension on Sox9 gene expression. Interestingly, Sox9 mRNA expression was not altered by hypoxia (Fig. 5A). As shown in Fig. 5B, Sox9 transcriptional activity was clearly up-regulated by BMP-2. However, it was not up-regulated but rather was down-regulated by hypoxia. Sox9 transcriptional activity has been reported to be enhanced by cAMP-dependent protein kinase A serine/threonine phosphorylation (63). We found that phosphorylation of Sox9 was not promoted but was suppressed by hypoxia (Fig. 5C), which was consistent with the results of the reporter assay.

**Runx2 Gene Expression and Its Transcriptional Activity Are Suppressed by Hypoxia**—Since hypoxia suppressed chondrocyte hypertrophy and osteoblastic differentiation, we studied the role of Runx2 in the regulation of hypoxia-induced phenomena. Hypoxia suppressed *Runx2* gene expression and its transcriptional activity in C3H10T1/2 cells stimulated with BMP-2 (Fig. 5, D and E). Blockade of the p38 MAPK pathway did not alter the suppression of *Runx2* caused by hypoxia, but blockade of the Smad pathway abolished the effect of hypoxia. However, when both pathways were blocked, hypoxia could again suppress *Runx2* gene expression (Fig. 5D). This pattern is very similar to the regulatory pattern we found for the hypoxic regulation of *Col10a1* gene expression. To examine how Runx2 contributes to chondrocyte terminal differentiation in hypoxia, we transfected C3H10T1/2 cells with vector expressing wild type Runx2. When Runx2 was overexpressed, the *Runx2* transcriptional activity suppressed by hypoxia was remarkably up-regulated to a level comparable with that with normoxia (Fig. 5E). In addition, *Col10a1* gene expression that had been reduced by hypoxia recovered to a level that matched the level expressed under normoxic conditions with Runx2 overexpres-

**FIGURE 5. Gene expression and transcriptional activity of Sox9 (A-C) and Runx2 (D-F) under hypoxia.** A-1, C3H10T1/2 cells were stimulated with BMP-2 (500 ng/ml) for 5 days. Total RNA was extracted, and Northern blotting was done for Sox9. A-2, real time PCR for the Sox9 gene was performed. Data are shown as mean  $\pm$  S.E. ( $n = 3$ ) of the proportion ratio for Sox9 gene expression as compared with normoxia. N.S., not significant. B, C3H10T1/2 cells were co-transfected with 4Col2E-Luc and TK-Renilla reporter constructs. As a control, the rat chondrosarcoma cell line (RCS) was used. 12 h after transfection, cells were incubated with or without BMP-2 (500 ng/ml) for 5 days. Luciferase activity was measured and normalized by determining Renilla luciferase activity. Data are shown as mean  $\pm$  S.E. ( $n = 3$ ). \*,  $p < 0.0001$ ; N.S., not significant. C, C3H10T1/2 cells were cultured for 5 days and lysed. The cell lysate was immunoprecipitated with anti-phosphoserine and phosphothreonine antibodies and blotted with anti-Sox9 antibodies. D-1, 12 h after infection with WT-Smad6 adenovirus, the cells were stimulated with BMP-2 (500 ng/ml) in the absence or presence of 1  $\mu$ M FR167653. As a control, LacZ expression adenovirus (MOCK) was used. After 48 h, total RNA was extracted, and Northern blotting for the Runx2 gene was performed. N, normoxia; H, hypoxia. D-2, real time PCR for Runx2 gene was performed. Data are shown as mean  $\pm$  S.E. ( $n = 3$ ) of the proportion ratio for Runx2 gene expression as compared with normoxia. \*,  $p < 0.001$ ; N.S., not significant. □, normoxia; ■, hypoxia. E, C3H10T1/2 cells were co-transfected with 6Runx2E-Luc and TK-Renilla reporter constructs. As a control, the mouse osteoblast cell line (MC3T3-E1) was used. 24 h after transfection, cells were incubated with BMP-2 (500 ng/ml) for 2 days, and relative luciferase activity was measured and normalized by determining Renilla luciferase activity. Data are shown as mean  $\pm$  S.E. ( $n = 3$ ). \*,  $p < 0.05$ ; \*\*,  $p < 0.0002$ ; N.S., not significant. F, 24 h after transfection with wild type Runx2, the cells were stimulated with BMP-2 (500 ng/ml) and incubated under normoxia or hypoxia for 5 days. As a control, the cells were transfected with pGL3 promoter vector. Then Northern blotting for *Col10a1* genes was performed.

# Oxygen Tension Regulates Chondrocytes



sion (Fig. 5F). These data suggest that Runx2 mediates *Col10a1* gene suppression by hypoxia and that a third regulatory mechanism, independent of the Smad and the p38 MAPK pathways, is involved in the regulation by oxygen tension of *Runx2* gene expression.

**HDAC4 Is Expressed by Chondrocytes and Accumulates in the Nucleus under Hypoxia**—Recently, it was reported that HDAC4 inhibits chondrocyte hypertrophy by suppressing *Runx2* gene expression. HDAC4 has been reported to be expressed by chondrocytes in the prehypertrophic and hypertrophic zones (47). We could detect HDAC4 only in chondrocytic lineage cells (N1511 or C3H10T1/2) and almost not in osteoblastic cells (MC3T3-E1) (Fig. 6A). We furthermore confirmed that HDAC4 protein was expressed in the hypertrophic chondrocytes of the growth plate but not in proliferative chondrocytes (Fig. 6B). To elucidate whether HDAC4-*Runx2* regulation is involved in the hypoxic suppression of terminal differentiation, we first examined the effect of oxygen tension on HDAC4 activation. Our immunofluorescence study revealed that the expression pattern of HDAC4 changed from being located in the cytoplasm to being located in the nucleus when cells were incubated under hypoxic conditions (Fig. 6, C-1). Accordingly, HDAC4 protein expression in the nuclear extract by Western blotting was up-regulated after 24 h of hypoxic stimulation (Fig. 6, C-2).

**Inhibition of HDAC4 Up-regulates *Runx2* Gene Expression and Its Transcriptional Activity and Restores *Col10a1* Gene Expression That Is Decreased by Hypoxia**—To evaluate whether HDAC4 is involved in the hypoxic regulation of *Runx2* and *Col10a1* gene expression, we inhibited HDAC4 by RNA interference (Fig. 6D). The inhibition of HDAC4 partly restored the reduced *Runx2* gene expression that resulted from 2 days of hypoxia. On day 5, *Runx2* gene expression was clearly promoted by HDAC4 silencing regardless of oxygen level, and the hypoxia-induced suppression of *Runx2* expression was completely restored to that seen with normoxia (Fig. 6E). Consistent with these results, HDAC4 inhibition completely abolished the reduction of *Runx2* transcriptional activity caused by hypoxia (Fig. 6F). As a consequence, after 5 days of hypoxic stimulation, *Col10a1* gene expression that had been suppressed by hypoxia was also up-regulated by HDAC4 inhibition and recovered to the level seen with normoxia. These data strongly suggested that hypoxia activates HDAC4, which in turn suppresses *Runx2* activity and subsequently leads to the reduction of *Col10a1* gene expression.

## DISCUSSION

Murine mesenchymal C3H10T1/2 cells are pluripotent and differentiate into several lineages (19). BMP-2 and BMP-7 induce C3H10T1/2 cells to differentiate into osteoblasts, chondrocytes, and adipocytes; a low concentration favors adipocytes, and a high concentration favors chondrocytes and osteoblasts (18, 19, 64, 65). Thus, C3H10T1/2 cells are an appropriate model for studying the mechanisms of pluripotent mesenchymal cell commitment into a particular lineage. In the present study, we cultivated C3H10T1/2 cells in the presence or absence of recombinant human BMP-2 under normoxia or hypoxia. BMP-2 treatment and low oxygen tension synergistically induced GAG production and *Col2a1* gene expression and profoundly suppressed ALP activity and mineralization; they did not alter fat droplet production. These data indicate that hypoxia promoted chondrocytic commitment of the pluripotent C3H10T1/2 mesenchymal cells and inhibited osteoblastic differentiation. Our results are in accordance with previous reports, which describe that hypoxia enhances *Col2a1* and Aggrecan gene expression in C3H10T1/2 cells (66). To further investigate the role of oxygen tension in chondrocytic differentiation, we used a mouse embryo forelimb explant culture system. This system enables one to cultivate cartilage tissue under hypoxic conditions for up to 2 weeks without any interference from systemic, hormonal, or neuronal responses to the hypoxia that could affect cartilage metabolism while at the same time examining the effects of both environmental factors and cytokines on the endochondral ossification process. In organ cultures of wild type mice forelimbs at 14.5 days postcoitum, we found that hypoxia clearly induced the enlargement of the cartilage matrix area stained by Safranin-O, suggesting that hypoxia promoted cartilage matrix synthesis by chondrocytes during endochondral ossification. To confirm this, we cultured N1511 chondrocytes under hypoxic conditions and found that hypoxia induced N1511 cells to produce GAG. Our data indicate that hypoxia not only induced the commitment of pluripotent mesenchymal progenitors into a chondrocyte lineage but also activated the production by chondrocytes of cartilage matrix.

In the present study, hypoxia in the presence of BMP-2 clearly suppressed *Col10a1* mRNA expression in C3H10T1/2 cell culture and also in organ culture studies using tissues from wild type animals. This suggests that hypoxia suppresses the terminal differentiation of chondrocytes during endochondral

**FIGURE 6. With hypoxia, HDAC4 accumulates in the nucleus and down-regulates *Runx2* expression, *Runx2* transcriptional activity, and *Col10a1* gene expression.** A, nuclear and cytoplasmic extracts from C3H10T1/2, N1511, and MC3T3-E1 cells (mouse osteoblastic cells) were examined by Western blotting with anti-HDAC4 antibodies. Mixed lysate (nuclear extract (10  $\mu$ g) plus cytoplasmic extracts (10  $\mu$ g)) was blotted for  $\beta$ -actin for the control. B, immunohistochemical analysis for HDAC4 protein in normal mouse embryo humerus (embryonic day 14.5). Bars, 30  $\mu$ m. B-1, HDAC4 protein expression in hypertrophic chondrocytes, not in proliferative chondrocytes. B-2, negative control without primary antibody. C, nuclear translocation of HDAC4 protein by hypoxia. C-1, immunofluorescence staining for HDAC4 protein. After starvation for 24 h, C3H10T1/2 cells were stimulated with BMP-2 (500 ng/ml) and further incubated under normoxia or hypoxia for 1 h. Immunofluorescence staining was performed using anti-HDAC4 antibody (1:100) for 2 h followed by Alexa Fluor 488 for 30 min. Hoechst 33342 was used for nucleus staining. Bar, 12.5  $\mu$ m. C-2, nuclear and cytoplasmic extracts from C3H10T1/2 cells were harvested and examined by Western blotting with anti-HDAC4 antibodies. Proliferating cell nuclear antigen and  $\beta$ -actin acted as the internal loading control for nuclear and cytoplasmic fractions, respectively. N, normoxia; H, hypoxia. D, 24 h after transfection with siRNA for HDAC4, nuclear extracts from the cells were harvested and analyzed by Western blotting with anti-HDAC4 antibodies. Proliferating cell nuclear antigen acted as the internal loading control for nuclear fractions. After transfection with siRNA for HDAC4, the cells were incubated for 5 days, and reverse transcription-PCR analysis for *Runx2* was done. E, 24 h after transfection with siRNA for HDAC4, the cells were stimulated by 500 ng/ml BMP-2 for either 48 h or 5 days. Northern blotting for *Runx2* and *Col10a1* were done. F, C3H10T1/2 cells were co-transfected with siRNA, 6*Runx2E-Luc*, and TK-*Renilla* reporter constructs. 24 h after transfection, cells were incubated with BMP-2 (500 ng/ml) for 48 h under normoxia or hypoxia. At the end of the culture, relative luciferase activity was determined. Data are shown as mean  $\pm$  S.E. ( $n = 3$ ). \*,  $p < 0.05$ ; N.S., not significant.

## Oxygen Tension Regulates Chondrocytes

ossification. Thus, hypoxia seems to act on chondrocytes to preserve their chondrocyte phenotype by preventing hypertrophy and, consequently, terminal differentiation.

To confirm the mechanisms by which these hypoxia-induced phenomena operate, we studied the signaling pathways of BMP-2 that are well known to induce chondrogenesis of mesenchymal cells (17–21) via the induction of *Sox9* gene expression (67). Basically, BMP-2 signals propagate through the Smad pathway and bind directly or via other DNA-binding proteins to the promoters of BMP-2-responsive genes to stimulate or repress their transcription. Over the past few years, evidence has accumulated that suggests that BMP-2 may also stimulate other downstream pathways involving p38 MAPK. In the present study, we found that hypoxia enhanced BMP-2-induced activation of the p38 MAPK pathway, whereas hypoxia did not promote and could even suppress the Smad pathway. Furthermore, our Smad- and p38 MAPK-suppressing studies using WT-Smad6, DN-MKK3, and FR167653 revealed that it is not the Smad pathway but the p38 MAPK pathway that is indispensable for hypoxia-induced cartilaginous matrix synthesis. Overall, our data indicate that hypoxia promotes cartilaginous matrix synthesis via the p38 MAPK pathway.

Little is known about how oxygen tension regulates the signal transduction systems that regulate *Col10a1* gene expression. In the present study, we found that hypoxia promoted BMP-2-induced activation of the p38 MAPK pathway but did not promote, and could even suppress, the Smad pathway. Previous reports suggested that Smad1-Smad5 signaling positively regulates type X collagen expression by potentiating the transcriptional activity of Runx2 (44, 45) and that p38 MAPK signaling also promotes its expression (34, 45, 68) via Runx2 activation. These observations are consistent with the results of our experiments that blocked these pathways by Smad6, DN-MKK3, or the p38 inhibitor, FR167653. This suggests that hypoxia positively regulates *Col10a1* gene expression via the up-regulation of p38 MAPK signaling and negatively regulates *Col10a1* gene expression via down-regulation of the Smad pathway. In addition to this, we found that hypoxia up-regulated HDAC4 activity, which recently was reported to control chondrocyte hypertrophy by suppressing *Runx2* gene expression through inhibition of the gene's positive feedback mechanism and the suppression of its transcriptional activity (47). We were able to confirm that hypoxic suppression of *Runx2* gene expression, transcriptional activity, and *Col10a1* gene expression were blocked by silencing HDAC4. This indicates that hypoxia activates HDAC4, thereby suppressing *Runx2* activity, which in turn down-regulates *Col10a1* gene expression. Our data reveal that hypoxia inhibits the hypertrophy of chondrocytes by down-regulating *Runx2* activity based on the sum of the positive regulation that occurs via p38 MAPK activation and the negative regulation that is caused by Smad signaling suppression and HDAC4 activation.

Transcriptional factors Sox9, L-Sox5, and Sox6, have been reported to be essential and sufficient for regulating the expression of *Col2a1* and the other genes involved in the chondrocytic program (69). This would suggest that Sox transcriptional factors should be up-regulated by hypoxia and thus propagate the signals for chondrocytic differentiation and cartilage matrix

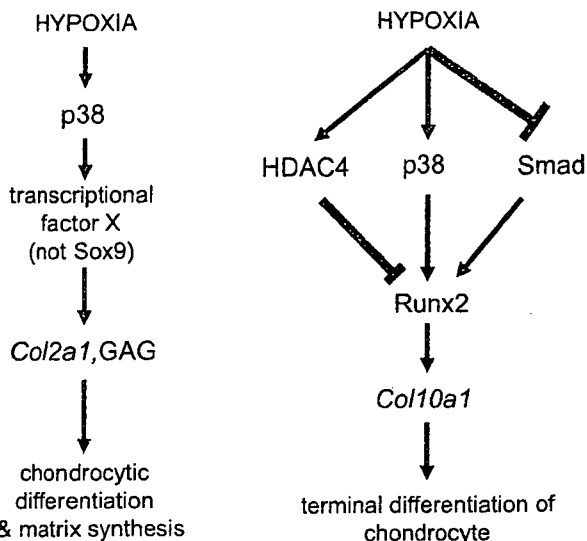


**FIGURE 7. Proposed models of the regulatory mechanisms responsible for chondrocyte differentiation and function based on oxygen level.** Hypoxia enhances the p38 MAPK pathway and suppresses the Smad pathway. Activated p38 MAPK signaling promotes *Col2a1* gene expression and GAG production independently of the Smad pathway and *Sox9*. Hypoxia inhibits *Col10a1* gene expression by reducing *Runx2* activity based on the sum of the positive regulation via p38 MAPK activation and the negative regulation caused by Smad signaling suppression and HDAC4 activation.

production. However, very interestingly, our results indicate that hypoxia-mediated chondrocytic differentiation did not involve the up-regulation of *Sox9* gene expression, its phosphorylation, or its transcriptional activity, suggesting that hypoxia-induced *Col2a1* induction was independent of *Sox9*. However, in the previous report, it was described that *Sox9* gene expression was up-regulated by hypoxia in association with transactivation of the *Sox9* promoter in ST2 stromal cells (66). Although the difference in the results might depend on the difference in cell type, further confirmation about the *Sox9* promoter may be necessary. The results of the reporter assay lead us to speculate that transcription factors other than *Sox9* directly regulate *Col2a1* gene expression via other cis elements located at a site other than the chondrocyte-specific enhancer fragment of the *Col2a1* gene (69, 70). The Sox trio shares a cis element in the *Col2a1* chondrocyte-specific enhancer region; however, to exclude the involvement of L-Sox5 and Sox6 in hypoxia-induced *Col2a1* gene expression, further confirmation, including gene expression of these transcription factors, is needed. It is known that hypoxic stress reduces protein kinase A activity (71). Recently, protein kinase A was reported to phosphorylate *Sox9* and to enhance its transcriptional activity (62). Taking these data into account, it is plausible that *Sox9* transcriptional activity could have been down-regulated by hypoxia. However, the actual transcription factors responsible for hypoxia-induced *Col2a1* induction remain to be elucidated (Fig. 7).

In conclusion, we demonstrated that hypoxia clearly promoted chondrocytic commitment of cells in the mesenchymal lineage, as well as cartilaginous matrix synthesis, and inhibited terminal differentiation both in cell culture and organ culture. These effects were primarily mediated by p38 MAPK activation

independent of Sox9. On the other hand, hypoxia inhibited the hypertrophy of chondrocytes via the down-regulation of Runx2 activity through Smad signaling suppression and HDAC4 activation. These hypoxia-induced phenomena affect mesenchymal cell differentiation and endochondral ossification by enhancing and preserving the chondrocytic phenotype and cell function, as well as preventing chondrocytes from terminal differentiation that subsequently leads to matrix degeneration and chondrocyte apoptosis. The hypoxia-associated regulation of chondrocytes that has been outlined in our study may be of fundamental importance in the biology and pathology of cartilage tissues and may be involved in endochondral ossification in the growth plate, in joint cartilage homeostasis, and in the etiology of osteoarthritis.

**Acknowledgments**—We thank Dr. Riko Nishimura for valuable comments on this work and for donating the dominant negative MKK3 vector and the wild type Smad6 expression adenovirus; Dr. Toshihisa Komori for donating the wild type Runx2 expression vector; and Dr. Hideto Watanabe and Dr. Nobuhiro Kamiya for donating the N1511 cells. We also thank Kaori Sudo for excellent technical assistance and Astellas Pharmaceutical Co. Ltd. for supplying recombinant human BMP-2 and FR167653.

## REFERENCES

- Falchuk, K. H., Goetzl, E. J., and Kulka J. P. (1970) *Am. J. Med.* **49**, 223–231
- Olesen, L. L. (1970) *Arthritis Rheum.* **13**, 769–776
- Treuhart, P. S., and McCarthy, D. J. (1971) *Arthritis Rheum.* **14**, 475–484
- Silver, I. A. (1975) *Philos. Trans. R. Soc. Lond. B Biol. Sci.* **271**, 261–272
- Kiaer, T., Gronlund, J., and Sorensen, K. H. (1988) *Clin. Orthop. Relat. Res.* **229**, 149–155
- Ferrell, W. R., and Najafipour, H. (1992) *J. Physiol.* **449**, 607–617
- Lee, N. H., and Shapiro, I. M. (1974) *Calcif. Tissue Res.* **16**, 277–282
- Brighton, C. T., Kitajima, T., and Hunt, R. M. (1984) *Arthritis Rheum.* **27**, 1290–1299
- Martus, R. E. (1973) *Arthritis Rheum.* **16**, 646–656
- Otte, P. (1991) *Z. Rheumatol.* **50**, 304–312
- Lee, R. B., and Urban, J. P. G. (1997) *Biochem. J.* **321**, 95–102
- Hiraki, Y., Inoue, H., Iyama, K., Kamizono, A., Ochiai, M., Shukunami, C., Iijima, S., Suzuki, F., and Kondo, J. (1997) *J. Biol. Chem.* **272**, 32419–32426
- Scipani, E., Ryan, H. E., Didrickson, S., Kobayashi, T., Knight, M., and Johnson, R. S. (2001) *Genes Dev.* **15**, 2865–2876
- Johnstone, B., Hering, T. M., Caplan, A. I., Goldberg, V. M., and Yoo, J. U. (1998) *Exp. Cell Res.* **238**, 265–272
- Huang, C. Y., Reuben, P. M., Ippolito, G. D., Schiller, P. C., and Cheung, H. S. (2004) *Anat. Rec.* **278**, 428–436
- Bosnakovski, D., Mizuno, M., Kim, G., Ishiguro, T., Okumura, M., Iwanaga, T., Kadosawa, T., and Fujinaga, T. (2004) *Exp. Hematol.* **32**, 502–509
- Shukunami, C., Ohta, Y., Sakuda, M., and Hiraki, Y. (1998) *Exp. Cell Res.* **241**, 1–11
- Asahina, I., Sampath, T. K., and Hauschka, P. V. (1996) *Exp. Cell Res.* **222**, 38–47
- Wang, E. A., Israel, D. I., Kelly, S., and Luxenburg, D. P. (1993) *Growth Factors* **9**, 57–71
- Atkinson, B. L., Fantle, K. S., Benedict, J. J., Huffer, W. E., and Gutierrez-Hartmann, A. (1997) *J. Cell. Biochem.* **65**, 325–339
- Haas, A. R., and Tuan, R. S. (2000) *Methods Mol. Biol.* **137**, 383–389
- Heiden, C. H., Miyazono, K., and Dijke, P. (1997) *Nature* **390**, 465–471
- Massague, J., and Wotton, D. (2000) *EMBO J.* **19**, 1745–1754
- Iwasaki, S., Iguchi, M., Watanabe, K., Hosono, R., Tsujimoto, M., and Kohno, M. (1999) *J. Biol. Chem.* **274**, 26503–26510
- Kimura, N., Matsuo, R., Shibuya, H., Nakashima, K., and Taga, T. (2000) *J. Biol. Chem.* **275**, 17647–17652
- Lee, J. K., Kim, S. H., Lewis, E. C., Azam, T., Reznikov, L. L., and Dinarello, C. A. (2004) *Proc. Natl. Acad. Sci. U. S. A.* **25**, 8815–8820
- Subbaramaiah, K., Hart, J. C., Norton, L., and Dannenberg, A. J. (2000) *J. Biol. Chem.* **275**, 14838–14845
- Xia, Z., Dickens, M., Raigneaud, J., Davis, R. J., and Greenberg, M. E. (1995) *Science* **270**, 1326–1331
- Kawasaki, H., Morioka, T., Shimohara, S., Kimura, J., Hirano, T., Gotoh, Y., and Nishida, E. (1997) *J. Biol. Chem.* **272**, 18518–18521
- Ghatan, S., Larner, S., Kinoshita, Y., Hetman, M., Patel, L., Xia, Z., Youle, R. J., and Morrison, R. S. (2000) *J. Cell Biol.* **150**, 335–347
- Zhu, Y., Mao, X. O., Sun, Y., Xia, Z., and Greenberg, D. A. (2002) *J. Biol. Chem.* **277**, 22909–22914
- Watanabe, H., Caestecker, M. P., and Yamada, Y. (2001) *J. Biol. Chem.* **276**, 14466–14473
- Lim, Y. B., Kang, S. S., An, W. G., Lee, Y. S., Chun, J. S., and Sonn, J. K. (2003) *J. Cell. Biochem.* **88**, 713–718
- Zhen, X., Wei, L., Wu, Q., Zhang, Y., and Chen, Q. (2001) *J. Biol. Chem.* **276**, 4879–4885
- Kronenberg, H. M. (2003) *Nature* **423**, 332–336
- Olsen, B. R., Reginato, A. M., and Wang, W. (2000) *Annu. Rev. Cell Dev. Biol.* **16**, 191–220
- Inada, M., Yasui, T., Nomura, S., Miyake, S., Deguchi, K., Himeno, M., Sato, M., Yamagiwa, H., Kimura, T., Yasui, N., Ochi, T., Endo, N., Kitamura, Y., Kishimoto, T., and Komori, T. (1999) *Dev. Dyn.* **214**, 279–290
- Kim, I. S., Otto, F., Zabel, B., and Mundlos, S. (1999) *Mech. Dev.* **80**, 159–170
- Takeda, S., Bonnamy, J. P., Owen, M. J., Ducey, P., and Karsenty, G. (2001) *Genes Dev.* **15**, 467–481
- Yoshida, C. A., Yamamoto, H., Fujita, T., Furuichi, T., Ito, K., Inoue, K., Yamana, K., Zanma, A., Takada, K., Ito, Y., and Komori, T. (2004) *Genes Dev.* **18**, 952–963
- Zheng, Q., Zhou, G., Morello, R., Chen, Y., Garcia-Rojas, X., and Lee, B. (2003) *J. Cell Biol.* **162**, 833–842
- Komori, T., Yagi, H., Nomura, S., Yamaguchi, A., Sasaki, K., Deguchi, K., Shimizu, Y., Bronson, R. T., Gao, Y. H., Inada, M., Sato, M., Okamoto, R., Kitamura, Y., Yoshiki, S., and Kishimoto, T. (1997) *Cell* **89**, 755–764
- Otto, F., Thornell, A. P., Crompton, T., Denzel, A., Gilmour, K. C., Rosewell, I. R., Stamp, G. W., Beddington, R. S., Mundlos, S., Olsen, B. R., Selby, P. B., and Owen, M. J. (1997) *Cell* **89**, 765–771
- Leboy, P., Grasso-Knight, G., D'Angelo, M., Volk, S. W., Lian, J. V., Drissi, H., Stein, G. S., and Adams, S. L. (2001) *J. Bone Joint Surg. Am.* **83**, Suppl. 1, S15–S22
- Drissi, M. H., Li, X., Sheu, T. J., Zuscik, M. J., Schwarz, E. M., Puzas, J. E., Rosier, R. N., and O'Keefe, R. J. (2003) *J. Cell. Biochem.* **90**, 1287–1298
- Mengshol, J. A., Vincenti, M. P., and Brinckerhoff, C. E. (2001) *Nucleic Acids Res.* **29**, 4361–4372
- Vega, R. B., Matsuda, K., Oh, J., Barbosa, A. C., Yang, X., Meadows, E., McAnally, J., Pomajzi, C., Shelton, J. M., Richardson, J. A., Karsenty, G., and Olsen, E. N. (2004) *Cell* **119**, 555–566
- Park, J. H., Park, B. H., Kim, H. K., Park, T. S., and Baek, H. S. (2002) *Mol. Cell. Endocrinol.* **192**, 197–203
- Kamiya, N., Jikko, A., Kimata, K., Damsky, C., Shimizu, K., and Watanabe, H. (2002) *J. Bone Miner. Res.* **17**, 1832–1842
- Lim, Y. B., Kang, S. S., Park, T. K., Lee, Y. S., Chun, J. S., and Sonn, J. K. (2000) *Biochem. Biophys. Res. Commun.* **273**, 609–613
- Ratisoontorn, C., Seto, M. L., Broughton, K. M., and Cunningham, M. L. (2005) *Bone* **36**, 627–634
- Sen, A., Lea-Currie, Y. R., Sujkowska, D., Franklin, D. M., Wilkison, W. O., Halvorsen, Y. D., and Gimble, J. M. (2001) *J. Cell. Biochem.* **26**, 312–319
- Horiki, M., Imamura, T., Okamoto, M., Hayashi, M., Murai, J., Myoui, A., Ochi, T., Miyazono, K., Yoshikawa, H., and Tsumaki, N. (2004) *J. Cell Biol.* **165**, 433–445
- Lanske, B., Karaplis, A. C., Lee, K., Luz, A., Volkamp, A., Pirro, A., Karpierien, M., Defize, L. H., Ho, C., and Mulligan, R. C. (1996) *Science* **273**, 663–666



## Oxygen Tension Regulates Chondrocytes

55. Vorkamp, A., Lee, K., Lanske, B., Segre, G. V., Kronenberg, H. M., and Tabin, C. J. (1996) *Science* **273**, 613–622
56. Minina, E., Kresche, C., Naski, M. C., Ornitz, D. M., and Vorkamp, A. (2002) *Dev. Cell* **3**, 439–449
57. Conlon, R. A., and Herrmann, B. G. (1993) *Methods Enzymol.* **225**, 373–383
58. Lefebvre, V., Zhou, G., Mukhopadhyay, K., Smith, C. N., Zhaoping, Z., Eberspaecher, H., Zhou, X., Sinha, S., Maity, S. N., and de Crombrugge, B. (1996) *Mol. Cell Biol.* **16**, 4512–4523
59. Chauchereau, A., Mathieu, M., de Saintignon, J., Ferreira, R., Pritchard, L. L., Mishal, Z., Dejean, A., and Harel-Bellan, A. (2004) *Oncogene* **23**, 8777–8784
60. Ito, K., Hanazawa, T., Tomita, K., Barnes, P. J., and Adcock, I. M. (2004) *Biochem. Biophys. Res. Commun.* **315**, 240–245
61. Schmid, T. M., and Linsenmayer, T. F. (1983) *J. Biol. Chem.* **258**, 9504–9509
62. Gibson, G. J., and Flint, M. H. (1985) *J. Cell Biol.* **101**, 277–284
63. Huang, W., Zhou, X., Lefebvre, V., and de Crombrugge, B. (2000) *Mol. Cell Biol.* **20**, 4149–4158
64. Katagiri, T., Yamaguchi, A., Ikeda, T., Yoshiki, S., Wozney, J. M., Rosen, V., Wang, E. A., Tanaka, H., Omura, S., and Suda, T. (1990) *Biochem. Biophys. Res. Commun.* **172**, 295–299
65. Ahrens, M., Ankenbauer, T., Schroder, D., Hollnagel, A., Mayer, H., and Gross, G. (1993) *DNA Cell Biol.* **12**, 871–880
66. Robins, J. C., Akeno, N., Mukherjee, A., Dalal, R. R., Arnow, B. J., Koopman, P., and Clemens, T. L. (2005) *Bone* **37**, 313–322
67. Lefebvre, V., Huang, W., Harley, V. R., Goodfellow, P. N., and de Crombrugge, B. (1997) *Mol. Cell Biol.* **17**, 2336–2346
68. Beitner-Johnson, D., Leibold, J., and Millhorn, D. E. (1998) *Biochem. Biophys. Res. Commun.* **242**, 61–66
69. Zehentner, B. K., Dony, C., and Burtscher, H. (1999) *J. Bone Miner. Res.* **14**, 1734–1741
70. Beier, F., and Luvall, P. (1999) *Biochem. Biophys. Res. Commun.* **262**, 50–54
71. Lefebvre, V., Li, P., and de Crombrugge, B. (1998) *EMBO J.* **17**, 5718–5733

Research article



## Enhanced expression of mRNA for nuclear factor $\kappa$ B1 (p50) in CD34+ cells of the bone marrow in rheumatoid arthritis

Shunsei Hirohata<sup>1</sup>, Yasushi Miura<sup>2</sup>, Tetsuya Tomita<sup>3</sup>, Hideki Yoshikawa<sup>3</sup>, Takahiro Ochi<sup>4</sup> and Nicholas Chiorazzi<sup>5</sup>

<sup>1</sup>Department of Internal Medicine, Teikyo University School of Medicine, Tokyo 173-8605, Japan

<sup>2</sup>Department of Rheumatology, Kobe University FHS School of Medicine, Kobe 654-0142, Japan

<sup>3</sup>Department of Orthopedic Surgery, Osaka University Medical School, Osaka 565-0871, Japan

<sup>4</sup>Sagamihara National Hospital, Kanagawa 228-8522, Japan

<sup>5</sup>Experimental Immunology and Rheumatology, North Shore-LIJ Research Institute, Manhasset, NY 11030, USA

Corresponding author: Shunsei Hirohata, [shunsei@med.teikyo-u.ac.jp](mailto:shunsei@med.teikyo-u.ac.jp)

Received: 1 Oct 2005 Revisions requested: 8 Nov 2005 Revisions received: 27 Jan 2005 Accepted: 9 Feb 2006 Published: 6 Mar 2006

*Arthritis Research & Therapy* 2006, **8**:R54 (doi:10.1186/ar1915)

This article is online at: <http://arthritis-research.com/content/8/2/R54>

© 2006 Hirohata et al.; licensee BioMed Central Ltd.

This is an open access article distributed under the terms of the Creative Commons Attribution License (<http://creativecommons.org/licenses/by/2.0>), which permits unrestricted use, distribution, and reproduction in any medium, provided the original work is properly cited.

### Abstract

Bone marrow CD34+ cells from rheumatoid arthritis (RA) patients have abnormal capacities to respond to tumor necrosis factor (TNF)- $\alpha$  and to differentiate into fibroblast-like cells producing matrix metalloproteinase (MMP)-1. We explored the expression of mRNA for nuclear factor (NF) $\kappa$ B in RA bone marrow CD34+ cells to delineate the mechanism for their abnormal responses to TNF- $\alpha$ . CD34+ cells were purified from bone marrow samples obtained from 49 RA patients and 31 osteoarthritis (OA) patients during joint operations via aspiration from the iliac crest. The mRNAs for NF $\kappa$ B1 (p50), NF $\kappa$ B2 (p52) and RelA (p65) were examined by quantitative RT-PCR. The expression of NF $\kappa$ B1 mRNA in bone marrow CD34+ cells was significantly higher in RA than in OA, whereas there was no

significant difference in the expression of mRNA for NF $\kappa$ B2 and RelA. The expression of NF $\kappa$ B1 mRNA was not correlated with serum C-reactive protein or with the treatment with methotrexate or oral steroid. Silencing of NF $\kappa$ B1 by small interfering RNA abrogated the capacity of RA bone marrow CD34+ cells to differentiate into fibroblast-like cells and to produce MMP-1 and vascular endothelial growth factor upon stimulation with stem cell factor, granulocyte-macrophage colony stimulating factor and TNF- $\alpha$  without influencing their viability and capacity to produce  $\beta$ 2-microglobulin. These results indicate that the enhanced expression of NF $\kappa$ B1 mRNA in bone marrow CD34+ cells plays a pivotal role in their abnormal responses to TNF- $\alpha$  and, thus, in the pathogenesis of RA.

### Introduction

Rheumatoid arthritis (RA) is a chronic inflammatory disease characterized by hyperplasia of synovial lining cells, consisting of macrophage-like type A synoviocytes and fibroblast-like type B synoviocytes [1]. It has been appreciated that type A synoviocytes, which are also called intimal macrophages, are derived from monocyte precursors in the bone marrow [1]. On the other hand, type B synoviocytes, which are also called fibroblast-like synoviocytes, have the morphological appearance of fibroblasts as well as the capacity to produce and secrete a variety of factors, including proteoglycans, cytokines, arachidonic acid metabolites, and matrix metallo-

proteinases (MMPs), that lead to the destruction of joints [1]. Apart from type A synoviocytes, the origin of type B synoviocytes has been unclear [1]. Of note, we have recently demonstrated that bone marrow CD34+ cells from RA patients have abnormal capacities to respond to tumor necrosis factor (TNF)- $\alpha$  and to differentiate into fibroblast-like cells producing MMP-1, suggesting that bone marrow CD34+ progenitor cells might generate type B synoviocytes and thus could play an important role in the pathogenesis of RA [2].

TNF- $\alpha$  is one of the first triggers to be found effective for the activation of nuclear factor (NF) $\kappa$ B in RA synovium [3]. This

$\beta$ <sub>2</sub>MG =  $\beta$ <sub>2</sub>-microglobulin; ELISA = enzyme-linked immunosorbent assay; GM-CSF = granulocyte-macrophage colony stimulating factor; HSCT = hematopoietic stem cell transplantation; MFI = mean fluorescence intensity; MMP = matrix metalloproteinase; MTX = methotrexate; NF $\kappa$ B = nuclear factor kappa B; OA = osteoarthritis; PCR = polymerase chain reaction; PE = phycoerythrin; RA = rheumatoid arthritis; SCF = stem cell factor; siRNA = small interfering RNA; TNF- $\alpha$  = tumor necrosis factor-alpha; VEGF = vascular endothelial growth factor.

mechanism of activation was followed by up-regulation of several inflammatory genes usually found in active RA. Accordingly, a number of studies have shown that TNF- $\alpha$  blockade has beneficial effects in the treatment of RA [4]. Moreover, inhibition of NF $\kappa$ B by the antioxidant N-acetylcysteine significantly reduced TNF- $\alpha$ - and NF $\kappa$ B-dependent gene expression and synovial proliferation [3]. We thus hypothesized that abnormal responses of RA bone marrow CD34+ cells to TNF- $\alpha$  might result from abnormal expression of NF $\kappa$ B genes. The current studies were undertaken, therefore, to explore the expression of mRNA for various components of NF $\kappa$ B in bone marrow CD34+ cells in RA.

## Materials and methods

### Patients and samples

Bone marrow samples were obtained from 49 patients with RA (8 males and 41 females; mean age, 58.6 years; age range, 35 to 78 years) who satisfied the American College of Rheumatology 1987 revised criteria for RA [5] and gave informed consent in accordance with the World Medical Association Declaration of Helsinki Ethical Principles for Medical Research Involving Human Subjects. The samples were taken during joint operations via aspiration from the iliac crest under anesthesia. As a control, bone marrow samples were similarly obtained from 31 patients with osteoarthritis (OA; 3 males and 28 females; mean age, 71.2 years; age range, 49 to 81 years) who gave informed consent. Most patients with RA and OA were taking non-steroidal anti-inflammatory drugs. Of the 45 patients with RA, 23 were treated with low dose methotrexate (MTX) and 33 were taking oral steroids when bone marrow samples were obtained. No OA patients were taking MTX or oral steroid.

### Preparation of bone marrow CD34+ cells

Mononuclear cells were isolated by centrifugation of heparinized bone marrow aspirates over sodium diatrizoate-Ficoll gradients. CD34+ cells were purified from the mononuclear cells by positive selection with magnetic beads (CD34 progenitor cell selection system; Dynal, Oslo, Norway). The cells thus prepared were >95% CD34+ cells and <0.5% CD19+ B cells, as previously described [2]. In addition, CD34+ cells derived from bone marrow aspirates from the iliac crests of healthy individuals (purity >95%) were purchased from BioWhittaker (Walkersville, MD, USA).

### RNA isolation and real-time quantitative PCR

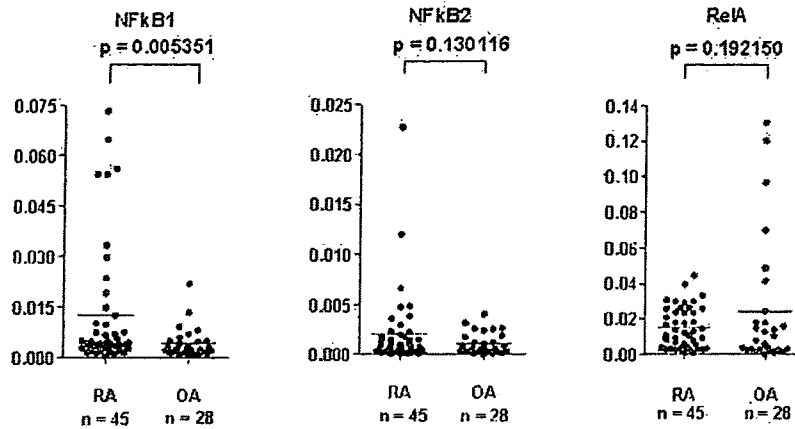
Total RNA was isolated from purified bone marrow CD34+ cells using the Trizol reagent (Life Technologies, Grand Island, NY, USA) according to the manufacturer's instructions. cDNA samples were prepared from 1  $\mu$ g of total RNA using the SuperScript reverse transcriptase preamplification system (Life Technologies) with oligo (dT) primer and subjected to PCR. Real-time quantitative PCR was performed using the LightCycler rapid thermal cycler system (Roche Diagnostics, Lewes, UK) with primer sets for NF $\kappa$ B1, NF $\kappa$ B2, RelA or  $\beta$ -actin and Light Cycler-Fast Start DNA master SYBR Green I (Roche Diagnostics). The primers were designed using Oligo Primer Analysis Software version 5.0 (Takara Bio Inc., Ohtsu, Japan). The detail of primer sequences is shown in Table 1. Quantitative analysis was performed using LightCycler Software v.3.5. PCR reaction conditions composed of denaturing at 95°C for 10 minutes for 1 cycle, followed by 40 cycles of denaturing (10 seconds at 95°C), annealing (10 seconds at 60°C (NF $\kappa$ B2, RelA) or 62°C (NF $\kappa$ B1,  $\beta$ -actin)), and extension (5 seconds (NF $\kappa$ B1), 6 seconds (NF $\kappa$ B2, RelA), or 10 seconds ( $\beta$ -actin) at 72°C).

Table 1

#### Primer sequences used in real-time quantitative PCR for analysis of mRNA for various nuclear factor $\kappa$ B components

Gene product (GenBank accession no.)	Primer sequences	Nucleotides
NF $\kappa$ B1 [M58603]	Forward: 5'-TCC ACA AGG CAG CAA ATA GA-3' Reverse: 5'-GGG GCA TTT TGT TGA GAG TT-3'	3,125-3,144 3,244-3,263
NF $\kappa$ B2 [NM_002502]	Forward: 5'-TTC TGA AGG CTG GTG CTG AC-3' Reverse: 5'-AGT GAG GTC AAG AGG CGT GT-3'	2,220-2,239 2,352-2,371
RelA [NM_021925]	Forward: 5'-GAA GAA GAG TCC TTT CAG CG-3' Reverse: 5'-GGG AGG ACG TAA AGG GAT AG-3'	1,011-1,030 1,116-1,135
$\beta$ -actin [X00351]	Forward: 5'-GCA AAG ACC TGT ACG CCA AC-3' Reverse: 5'-CTA GAA GCA TTT GCG GTG GA-3'	910-929 1,150-1,169

Figure 1



The expression of mRNAs for nuclear factor (NF) $\kappa$ B1 (p50), NF $\kappa$ B2 (p52) and RelA (p65) in bone marrow CD34<sup>+</sup> cells. Total RNA was isolated from purified bone marrow CD34<sup>+</sup> cells. The expression of mRNAs for NF $\kappa$ B1, NF $\kappa$ B2, RelA and  $\beta$ -actin was evaluated by real-time quantitative PCR. The data are expressed as the ratio of the mRNA copy numbers to those of  $\beta$ -actin. Horizontal lines indicate the mean values. Statistical significance was evaluated by Welch's *t* test. OA, osteoarthritis; RA, rheumatoid arthritis.

#### Immunofluorescence staining and analysis

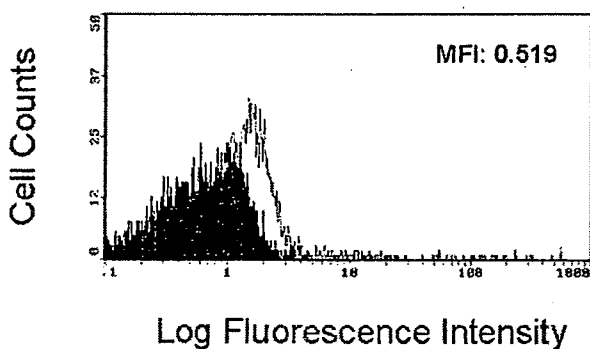
Purified bone marrow CD34<sup>+</sup> cells (obtained from three RA patients and three OA patients) were treated with IntraPrep™ Permeabilization Reagent (Immunotech, Marseille, France), followed by staining with phycoerythrin (PE)-conjugated anti-NF $\kappa$ B p50 (E-10; a mouse IgG1 monoclonal antibody against amino acids 120 to 239 mapping at the amino terminus of human NF $\kappa$ B p50; Santa Cruz Biotech, Santa Cruz, CA, USA) or PE-conjugated normal mouse IgG1 (Santa Cruz). The cells were analyzed using an EPICS XL flow cytometer (Coulter, Hialeah, FL, USA) equipped with an argon-ion laser at 488 nm. A combination of low-angle and 90° light scatter measurements (forward scatter versus side scatter) was used to gen-

erate a bit map gating to identify bone marrow cells using Cyto-Trol™ Control Cells (Coulter) and Immuno-Trol™ Cells (Coulter) as standards. Specific mean fluorescence intensity (MFI) for NF $\kappa$ B1 (p50) was calculated by subtracting the non-specific MFI of staining with the isotype-matched control mouse IgG1.

#### Culture medium and cytokines

RPMI 1640 medium (Life Technologies) supplemented with L-glutamine (0.3 mg/ml) and 10% fetal bovine serum (Life Technologies) was used for all cultures. Recombinant human stem cell factor (SCF), granulocyte-macrophage colony stimulating factor (GM-CSF), and TNF- $\alpha$  were purchased from Pepro Tech EC (London, UK).

Figure 2



Expression of nuclear factor (NF) $\kappa$ B1 (p50) protein in bone marrow CD34<sup>+</sup> cells. Purified bone marrow CD34<sup>+</sup> cells from a rheumatoid arthritis patient were permeabilized and then stained with phycoerythrin-conjugated anti-NF $\kappa$ B p50 monoclonal antibody or phycoerythrin-conjugated normal mouse IgG1, followed by analysis with flow cytometry. The level of NF $\kappa$ B1 protein was expressed by mean fluorescence intensity as described in Materials and methods.

#### Silencing of NF $\kappa$ B1 in bone marrow CD34<sup>+</sup> cells by small interfering RNA

SMARTpool® small interfering RNA (siRNA) for NF $\kappa$ B1 (p50) gene and nonsense scrambled control siRNA were purchased from Dharmacon (Lafayette, CO, USA). Chemical transfection of siRNAs into bone marrow CD34<sup>+</sup> cells was performed using siPORT™ Amine Transfection Agent (Ambion, Austin, TX, USA) according to the manufacturer's directions. Briefly, purified bone marrow CD34<sup>+</sup> cells were cultured in a 24-well microtiter plate (NO. 3524; Costar, Cambridge, MA, USA) at  $2 \times 10^5$  cells per well in 0.2 ml culture medium in the presence of SCF (10 ng/ml) and GM-CSF (1 ng/ml). After 24 hours of incubation, chemical transfection of siRNAs was performed, and incubated for 4 hours.

#### Cell cultures and measurement of MMP-1 and vascular endothelial growth factor

After transfection of siRNAs, the cells were cultured with SCF (10 ng/ml) and GM-CSF (1 ng/ml) in 1.0 ml culture medium for